

Interface Design and Development of Coating Materials in Lithium–Sulfur Batteries

Xia Li and Xueliang Sun*

High-energy Li-S batteries have received extensive attention and are considered to be the most promising next-generation electric energy storage devices beyond Li-ion batteries. Interface design is an important direction to address challenges in the development of Li–S batteries. This review summarizes recently developed coatings and interlayer materials at various interfaces of Li–S batteries. In particular, advanced nanostructures and novel fabrication methods of coating and interlayer materials applied to Li–S batteries are highlighted. Furthermore, underlying mechanisms at the interfaces and electrochemical performance of the developed Li–S batteries are also discussed. Finally, existing challenges and the future development of interface design in high-energy Li–S batteries are summarized and prospected.

1. Introduction

Lithium–sulfur batteries (Li–S batteries) are considered to be one of the most promising next-generation energy storage devices beyond Li-ion batteries.^[1] The ultrahigh specific energy density is an unparalleled advantage of Li–S batteries compared to other energy storage devices, and the economic price and environmental benignity of sulfur are also attractive properties.^[2] Due to these advantages, Li–S batteries are proposed for use in long-range electric vehicles (EVs) and hybrid electric vehicles (HEVs).^[3] Unfortunately, many challenges still hinder the development of Li–S batteries.

A typical Li–S battery is composed of a sulfur-based cathode, a lithium anode, a separator, and organic liquid electrolytes, as shown in **Figure 1a**. For cathodes, the insulating nature of sulfur and the lithium (di)sulfide discharge product is inimical to the electrochemical energy conversion, resulting in diminished utilization of sulfur in Li–S batteries.^[4] The dissolution of polysulfides is another serious issue pertinent to sulfur cathodes, often referred to as the “shuttle effect” of polysulfides, resulting in loss of active sulfur materials as well as corrosion of lithium metal.^[4a,b] Furthermore, the volume of a sulfur cathode can expand up to 80% during the conversion from S to Li₂S,

and the mechanical damage of electrode caused by the volume expansion induces a rapid decrease of battery capacity. In terms of the anode, most Li–S batteries still use lithium metal which poses challenges of both safety and performance in Li–S batteries.^[5] First, side reactions triggered by polysulfides and the surrounding electrolyte consume lithium metal quickly and form an insulated interlayer on the lithium metal, which damages the Li anode structure and blocks Li/Li⁺ transformation.^[2a,6] Second, similar to Li-ion batteries, lithium anodes suffer from the inevitable growth of lithium dendrites, which poses safety concerns in Li–S batteries.^[7] As a result, all of these challenges hinder the develop-


ment of high-energy Li–S batteries in practical applications.^[8]

A number of researchers and scientists have devoted relentless effort to address the challenges of Li–S batteries, such as the development of various carbon hosts, engineering the electrode structure, optimization of electrolytes, as well as coupling with high-energy anode materials.^[1c,2c,3c,9] Among the recent literature, the investigation and modification of interfaces via coating and interlayer materials are very promising and prevailing strategies in Li–S batteries.^[1c,2c,3c,10] As shown in **Figure 1b–d**, this review is divided into three parts based on different interface areas, which are the interfaces at i) sulfur cathodes, ii) separators, and iii) lithium anodes. Based on the issues at different interfaces, various design principles and requirements of coating and interlayer materials are developed. This review summarizes the study of interface design with coating and interlayer materials for Li–S batteries at different interfaces. The content covers structure design, synthetic approach, electrochemical performance, reaction mechanisms, as well as future perspectives of coating materials applied to Li–S batteries.

2. Interface Design on Sulfur-Based Cathodes in Li–S Batteries

Dissolution of polysulfides in organic liquid electrolytes and accompanied “shuttle effect” side reactions are severe challenges of cathode materials in Li–S batteries.^[18] One feasible solution is to cover the cathodes with a barrier to retain sulfur-based active materials,^[19] and such coating materials for sulfur cathodes are considered to be a favorable strategy. According to the features of these challenges, an ideal coating material for electrode materials should possess the following

Dr. X. Li, Prof. X. Sun
Department of Mechanical and Materials Engineering
University of Western Ontario
London, ON N6A 5B9, Canada
E-mail: xsun9@uwo.ca

 The ORCID identification number(s) for the author(s) of this article can be found under <https://doi.org/10.1002/adfm.201801323>.

DOI: 10.1002/adfm.201801323

characteristics:^[20] 1) uniform growth on target materials; 2) ultrathin layer thickness allowing smooth ion and electron diffusion; 3) high ionic conductivity for lithium ion transport; 4) good corrosion properties to sustain prolonged electrochemical reaction processes;^[21] and 5) high toughness to accommodate the large volume expansion during cycling.^[22] During the past decade, many advanced nanomaterials have been developed as coating materials for sulfur cathodes.^[23] According to the different target materials, we will introduce the coating and interlayer materials applied on cathode composites and on cathode electrodes in this section, respectively.

2.1. Development of Coating Materials for Sulfur/Li₂S-Based Composites

Following the use of highly ordered porous carbon reported by Nazar and co-workers,^[19b] numerous researchers have developed different kinds of carbon materials as hosts in sulfur cathodes.^[34] To some extent, encapsulating sulfur in hosts helps to relieve the “shuttle effect” in cycling. However, using host materials still cannot completely halt the dissolution of polysulfides into the electrolyte, thereby prompting researchers to develop coatings on sulfur-based composites to address this issue. According to the low melting (120 °C) and boiling temperature (≈400 °C) of sulfur, the synthesis of coating materials should be carried out under mild conditions with relatively low temperature. The coating materials should also meet a number of requirements including good electronic and ionic conductivities, chemical stability, and low specific weight. Therefore, carbon-based materials such as conductive polymers and 2D graphene are popular coatings applied to sulfur-based composites.

2.1.1. Polymer-Based Coating Materials

Conductive polymer materials have been developed over centuries and have been widely applied to Li-ion cathode and anode materials to improve the performance of batteries.^[35] The synthesis of polymer coatings mainly relies on chemical approaches, and mild synthetic processes are favorable to the uniform polymer growth on sulfur-based composites.^[36]

Early work of polymer coatings for sulfur cathodes was conducted by Wu et al. who reported the use of polythiophene as a coating material for core-shell sulfur/polythiophene composites.^[24] During the synthetic process, Fe³⁺ is used as a polymerizer to decorate the surface of sulfur particles and catalyze the thiophene monomer to polymerize on the surface of the sulfur particles, as shown in **Figure 2a**. Different ratios of the sulfur/polythiophene composites were characterized by elemental analysis. An optimized ratio for the composites was found to be 71.9% sulfur with 18.1% of polythiophene as determined by electrochemical results. The polythiophene coating layer acts as a conducting medium and a porous adsorbing agent for polysulfides, which brings improved cycling performance for Li-S batteries. The initial discharge capacity of the active material was 1119.3 mAh g⁻¹, with a capacity of 830.2 mA h g⁻¹ after



Xia Li is currently a postdoctoral fellow in Prof. Xueliang (Andy) Sun's Nanomaterials and Energy Group. She received her Bachelor degree in Chemical Engineering from Dalian University of Technology, China, in 2009 and Master degree in Materials Physics and Chemistry from Nankai University, China, in 2012. In 2016, she received her Ph.D. degree at the University of Western Ontario, Canada. Her current research interests focus on Li-S batteries, all-solid-state Li-ion and Li-S batteries, and battery interface studies via synchrotron X-ray characterizations.



Xueliang Sun is a Canada Research Chair in Development of Nanomaterials for Clean Energy, Fellow of the Royal Society of Canada and Canadian Academy of Engineering and Full Professor at the University of Western Ontario, Canada. He received his Ph.D. in materials chemistry in 1999 from the University of Manchester, UK, which he followed up by working as a postdoctoral fellow at the University of British Columbia, Canada. His current research interests are focused on advanced materials for electrochemical energy storage and conversion, including electrocatalysis in fuel cells and electrodes in lithium based batteries and metal-air batteries.

80 cycles. Later, Gao et al. used polyaniline (PANI) as a coating material to cover sulfur-mesoporous carbon composites.^[25] The research emphasized high rate performance of sulfur cathodes with the PANI coating due to a synergistic effect of the high electrical conductivity from both the conductive carbon black in the matrix and the PANI coating on the surface, as shown in **Figure 2b**. In the same year, Cui and co-workers reported the use of another conductive polymer, poly(3,4-ethylenedioxythiophene):poly(styrene sulfonate) (PEDOT:PSS) as a coating material on sulfur-ordered mesoporous carbon (S-CMK), as shown in **Figure 2c**.^[12] The battery performance and corresponding characterizations demonstrate that the conductive polymer PEDOT:PSS coating could be used to effectively trap polysulfides and minimize the loss of active sulfur material in cathodes, which leads to a remarkable improvement in the performance of Li-S batteries. Later, Cui and co-workers also investigated the three typical polymer coating materials, PEDOT, PANI, and

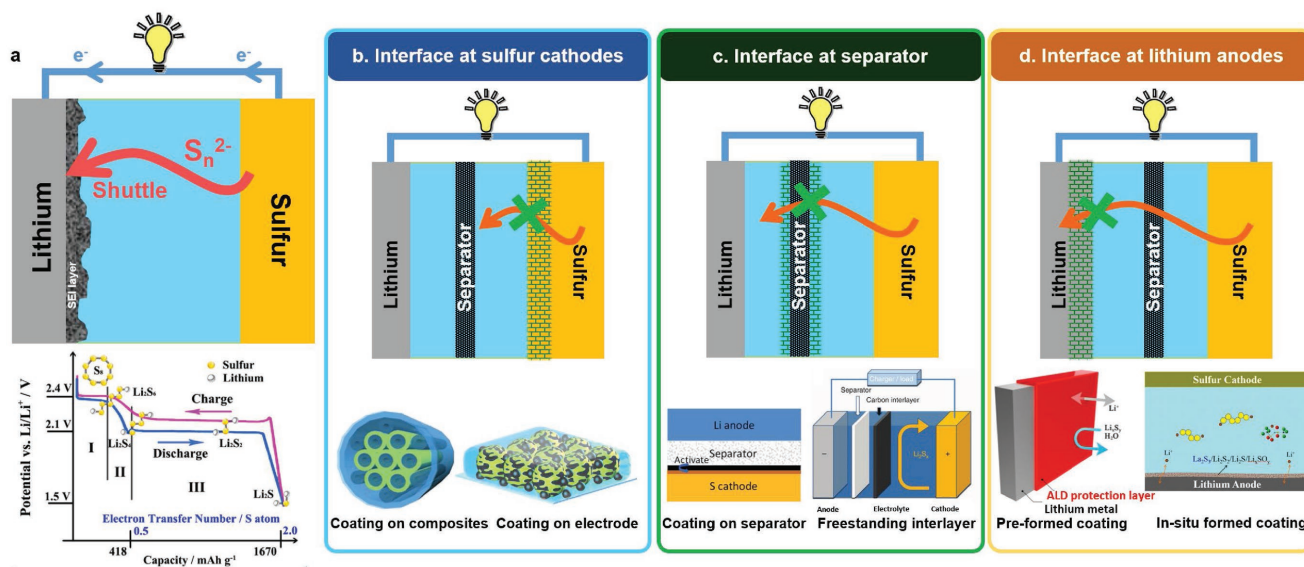


Figure 1. Schematic figure of Li-S batteries. a) Schematic configuration of a Li-S battery. Bottom: Reproduced with permission.^[11] Copyright 2016, Elsevier. b–d) Different interfaces designed for Li-S batteries summarized in this review. b) Interface at sulfur cathodes. Left: Reproduced with permission.^[12] Copyright 2011, American Chemical Society. Right: Reproduced with permission.^[13] Copyright 2016, American Chemical Society. c) Interface at separator. Left: Reproduced with permission.^[14] Copyright 2014, Royal Society of Chemistry. Right: Reproduced with permission.^[15] Copyright 2012, Nature Publishing Group. d) Interface at Li anodes. Left: Reproduced with permission.^[16] Copyright 2015, American Chemical Society. Right: Reproduced with permission.^[17] Copyright 2016, American Chemical Society.

polypyrrole (PPy), on sulfur-based composites and made a comparison of the electrochemical performance of the three coated sulfur cathodes in Li–S batteries.^[37] The study found that the capability of these three polymers in improving long-term cycling stability and high-rate performance of the sulfur cathodes decreased in the order of PEDOT > PPy > PANI. Following pioneering work, many other conductive polymers, such as pentaerythritol tetrakis (3-mercaptopropionate) (PETT), polydopamine (PDA), and Nafion, were also employed as coating materials for sulfur cathodes with improved electrochemical performance, as summarized in **Table 1**.^[38] The mild synthetic condition and in situ formation process of polymer coating materials promote their application to various sulfur-based composites, such as porous carbon–sulfur composites, multiwall carbon nanotubes–sulfur composites (MWCNTs–S), and graphene–sulfur composites.^[39] The most reported polymer-based coatings for sulfur cathodes act as both conductive agents and physical barriers to trap polysulfides. Furthermore, polymer coating materials can be designed to various nanostructures for sulfur cathodes. Taking carbon nanotube (CNTs) for instance, one polymer coating strategy is to cover the polymer coating on the surface of S–CNT composites.^[39] The CNTs with high aspect ratio, as substrates, provide a conductive path for sulfur, while the polymer coating helps to confine dissolved polysulfides and further improves the conductivity of the whole electrode. On the other hand, Wei and co-workers have reported another polymer coating structure that employs polyethylene glycol (PEG) coating as barrier layer at one end of aligned sulfur–CNT composites.^[40] The aligned CNT framework afforded high conductivity for electron transportation and ordered pores for lithium-ion transportation while the PEG barrier layer greatly suppressed the shuttle of polysulfides.

2.1.2. Graphene-Based Coating Materials

Since the discovery of graphene in 2004, this 2D carbon allotrope has been one of the most popular materials for the use in a variety of energy storage systems.^[41] The 2D structure, high conductivity, high surface area, as well as chemical and physical stability of graphene are very attractive properties as coating materials for sulfur cathodes.^[42]

The synthetic approaches for graphene coatings on sulfur-based composites are mainly chemical solution-based methods. Dai and co-workers first reported the use of graphene-wrapped sulfur particles as sulfur cathode materials for Li–S batteries.^[26] During the synthetic process, sulfur particles were first dispersed in solution and decorated by PEG, and then coated by a graphene oxide film, as shown in Figure 2d. The graphene coating layer is proposed to improve the conductivity of sulfur cathodes and trap polysulfides during electrochemical reactions. PEG is designed to accommodate the volume expansion from sulfur particles. The obtained graphene-wrapped sulfur composites thereby demonstrated significantly improved cycling stability with specific capacities of up to 600 mAh g⁻¹ over 100 cycles. In the same year, Evers and Nazar reported graphene-enveloped sulfur composites for Li–S batteries, as shown in Figure 2e.^[27] The research emphasized high Coulombic efficiency of prepared graphene–sulfur composites with high sulfur content (85 wt%). The author proposed that the graphene coating layer with highly graphitic and slightly hydrophilic properties has interactions with polysulfides via the oxo groups, which facilitate the absorption of polysulfides to stabilize the cycling performance of Li–S batteries.

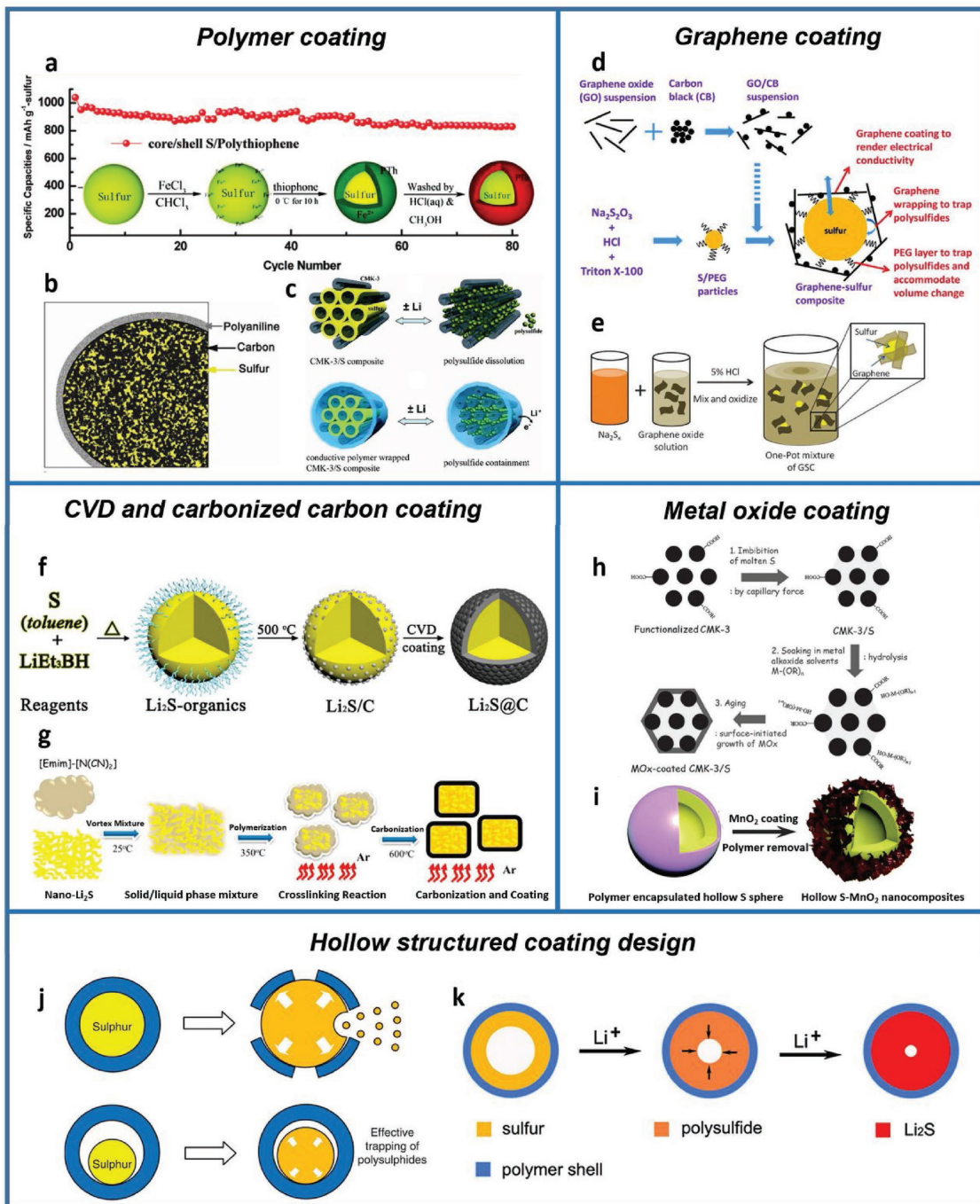


Figure 2. Different coating materials and nanostructure applied for sulfur/Li₂S composites. a) Reproduced with permission.^[24] Copyright 2011, American Chemical Society. b) Reproduced with permission.^[25] Copyright 2012, John Wiley & Sons, Inc. c) Reproduced with permission.^[12] Copyright 2011, American Chemical Society. d) Reproduced with permission.^[26] Copyright 2011, American Chemical Society. e) Reproduced with permission.^[27] Copyright 2012, Royal Society of Chemistry. f) Reproduced with permission.^[28] Copyright 2014, American Chemical Society. g) Reproduced with permission.^[29] Copyright 2015, Elsevier. h) Reproduced with permission.^[30] Copyright 2012, John Wiley & Sons, Inc. i) Reproduced with permission.^[31] Copyright 2016, Royal Society of Chemistry. j) Reproduced with permission.^[32] Copyright 2013, Nature Publishing Group. k) Reproduced with permission.^[33] Copyright 2013, National Academy of Sciences.

2.1.3. CVD Carbon Coating and High-Temperature Carbonization

Chemical vapor deposition (CVD) of carbon coatings is an alternative novel synthetic approach applied in Li-S batteries. Due to the high-temperature synthesis (>500 °C), this method

is mostly applied to Li₂S-based composites. Cairns and co-workers first reported the synthesis of carbon-coated Li₂S core-shell (Li₂S@C) particles via CVD, as shown in Figure 2f.^[28] The created Li₂S-carbon core-shell structure enables long cycling life and prevents polysulfide dissolution

Table 1. Summary of different coating materials applied for sulfur cathodes.

Coating materials		Sulfur content [wt%]	Sulfur loading	Coating thickness	Cycling performance	Ref.	
Coating materials applied to composites	Polymer	Polyaniline	43.7	1.21 mg cm ⁻²	10 nm	596 mAh g ⁻¹ (0.1 C 100 cycles)	[25]
			70	Not mentioned	20 nm	932 mAh g ⁻¹ (100 mA g ⁻¹ 80 cycles)	[39a]
			82	2 mg cm ⁻²	N/A	765 mAh g ⁻¹ (0.2 C, 200 cycles)	[61]
		Polydopamine	81	1.12 mg cm ⁻²	N/A	955 mAh g ⁻¹ (0.1 C 200 cycles)	[62]
			65	1.5 mg cm ⁻²	>200 nm	900 mAh g ⁻¹ (0.2 C, 150 cycles)	[45]
		Polyethylene-oxide	50	0.43 mg cm ⁻²	10 nm	600 mAh g ⁻¹ (0.5 C, 150 cycles)	[12]
		Polythiophene	71.9	Not mentioned	20–30 nm	830 mAh g ⁻¹ (100 mA g ⁻¹ , 80 cycles)	[24]
		Polypyrrole	50	Not mentioned	N/A	600 mAh g ⁻¹ (50 mA g ⁻¹ 20 cycles)	[63]
			63	0.63–1.26 mg cm ⁻²	100 nm	600 mAh g ⁻¹ (0.2 C, 50 cycles)	[64]
			48–60	Not mentioned	50 nm	880 mAh g ⁻¹ (0.2 C, 100 cycles)	[65]
	PETT-based polymer	Not mentioned	1.5–2 mg cm ⁻²	N/A	600 mAh g ⁻¹ (0.5 C, 200 cycles)	[66]	
		Nafion polymer	71.8	Not mentioned	N/A	≈750 mAh g ⁻¹ (0.1 C 50 cycle)	[67]
		Graphene	Graphene oxide	50	Not mentioned	N/A	800 mAh g ⁻¹ (1000 mA g ⁻¹ , 1000 cycles)
	Graphene wrapped sulfur–carbon fiber composites		33	0.4–0.6 mg cm ⁻²	N/A	694 mAh g ⁻¹ (0.1 C, 50 cycles)	[23c]
	Graphene wrapped sulfur particle		70	0.8–1.2 mg cm ⁻²	N/A	600 mAh g ⁻¹ (0.2 C, 100 cycles)	[26]
	CVD carbon coating	Li ₂ S@CVD carbon	88	1.1 mg cm ⁻²	30 nm	417 mAh g ⁻¹ (0.5 C, 400 cycles)	[28]
		Li ₂ S/GO@C	87	0.7–0.9 mg cm ⁻²	25 nm	584 mAh g ⁻¹ (2 C, 150 cycles)	[43]
		C-coated Li ₂ S nanoparticles on graphene	55	0.6–1.3 mg cm ⁻²	10 nm	750 mAh g ⁻¹ (0.5 C, 700 cycles)	[44b]
		Core–shell Li ₂ S@C	72.3	1.6 mg cm ⁻²	20 nm	766.4 mAh g ⁻¹ (0.2 C, 200 cycles)	[44c]
		3D high loading Li ₂ S@C	Not mentioned	7 mg cm ⁻²	15 nm	567.5 mAh g ⁻¹ (1 C, 200 cycles)	[68]
Other carbon coating	Carbon cage encapsulating Li ₂ S	91	1.5–1.8 mg cm ⁻²	5 nm	350 mAh g ⁻¹ (1 C, 500 cycles)	[29]	
	Carbon-coated core–shell Li ₂ S@C	92	10 mg cm ⁻²	0.8 nm	954 mAh g ⁻¹ (0.1 C, 100 cycles)	[44c]	
Metal oxides coating	Sulfur–TiO ₂ yolk–shell nanoarchitecture	71	0.4–0.6 mg cm ⁻²	15 nm	≈700 mAh g ⁻¹ (0.5 C, 1000 cycles)	[32]	
	MO _x -coated CMK-3/S (M = Si, V)	60–70	0.7–0.8 mg cm ⁻²	5 nm	500 mAh g ⁻¹ (0.1 C, 100 cycles)	[30]	
	TiO ₂ -coated mesoporous carbon–sulfur	53	Not mentioned	10 nm	608 mAh g ⁻¹ (0.2 C, 120 cycles)	[69]	
	MnO ₂ -coated hollow S nanocomposites	75.5	1.7–2.1 mg cm ⁻²	Not mentioned	1072 mAh g ⁻¹ (0.2 C, 200 cycles)	[31]	
	Coating materials and interlayer applied to electrode	Carbon-based coating layer	TiO ₂ /graphene interlayer	46.9	0.47 mg cm ⁻²	3 μm	1040 mAh g ⁻¹ (0.5 C, 300 cycles)
S–N dual doped graphene interlayer			68	0.56 mg cm ⁻²	4 μm	600 mAh g ⁻¹ (2 C, 250 cycles)	[49b]
Dendrimer-graphene oxide composite film			76	2 mg cm ⁻²	100 nm	698 mAh g ⁻¹ (1 C, 500 cycles)	[47]

Table 1. Continued.

	Coating materials	Sulfur content [wt%]	Sulfur loading	Coating thickness	Cycling performance	Ref.
	BP2000/PEDOT:PSS interlayer	75	2 mg cm ⁻²	100 nm	900 mAh g ⁻¹ (0.3 C, 200 cycles)	[48]
ALD and MLD coating	Plasma-enhanced ALD Al ₂ O ₃ coating	50	Not mentioned	3–5 nm	420 mAh g ⁻¹ (0.2 C, 400 cycles)	[51]
	ALD Al ₂ O ₃ coating on graphene–sulfur electrode	53	1 mg cm ⁻²	Not mentioned	650 mAh g ⁻¹ (0.5 C, 100 cycles)	[56b]
	ALD Al ₂ O ₃ coating on porous carbon–sulfur electrode	65	Not mentioned	0.4–2 nm	630 mAh g ⁻¹ (0.1 C, 70 cycles)	[56a]
	MLD alucone coating on porous carbon–sulfur electrode	65	Not mentioned	Not mentioned	710 mAh g ⁻¹ (0.1 C, 100 cycles)	[57]
	MLD alucone-coated carbon–sulfur in carbonate electrolyte	65	0.9 mg cm ⁻²	5.4 nm	600 mAh g ⁻¹ (0.1 C, 300 cycles, 55 °C)	[13]

with a high Li₂S content. Later, a unique conformal CVD carbon coating was also developed via a rotation quartz tube by Cairns and co-workers.^[43] An energy-filtered transmission electron microscope (EFTEM) with a selected energy window corresponding to the Li K-edge and C K-edge has demonstrated the conformal carbon coating with around 25 nm coating on Li₂S particles. The Li₂S/GO@C nanocomposite shows very low capacity fading with a reduction of only 0.046% per cycle over 1500 cycles. In addition to the CVD method, Wang and co-workers utilized ionic liquid (1-ethyl-3-methylimidazolium dicyanamide) as a carbon precursor to build a carbon cage on Li₂S nano-clusters, as shown in Figure 2g.^[29] The high-temperature carbonization strategy forms a dense carbon coating of within 5 nm on Li₂S active materials. Following these studies, many other groups also developed CVD carbon coatings and high-temperature carbonization coating materials on Li₂S composites, and the obtained cathode materials demonstrate stable and excellent performance in Li–S batteries, as shown in Table 1.^[44]

2.1.4. Metal Oxide Coating Materials

In addition to carbon-based materials, metal oxides are also employed as coating materials for sulfur cathodes. Nazar et al.^[30] developed surface initiated thin oxide coating materials via gas-phase repetitive sequential reactions, as shown in Figure 2h. The developed SiO_x and VO_x coatings have been demonstrated to be very thin layers (<5 nm) on CMK-3/S composites, indicating the well-controlled thickness of this thin-film coating approach. The developed sulfur cathodes demonstrate improved Coulombic efficiency and stabilized cycling performance. The author also mentioned the low conductivity of the metal oxide coatings, which directly affects the utilization of sulfur-active materials during cycling. Although the electronic conductivities of the reported metal oxides are limited,

the novel nanostructure and facile synthetic approaches are notable in the practical application of Li–S batteries and other energy storage systems. Another recent report by Chen et al. described a novel MnO₂ sheet coating on hollow sulfur spheres, as shown in Figure 2i.^[31] The developed MnO₂ coating film is attributed to trap Li_xS_n in chemical interactions and the spatial restriction of polysulfide dissolution which leads to the stabilized cycling performance of Li–S batteries. X-ray photoelectron spectra (XPS) of the core level of Mn and S elements have demonstrated the strong bonding between polysulfides and MnO₂. The density functional theory (DFT) calculations of the bonding energy between Li₂S_x and δ-MnO₂ nanosheet (100) surface further illustrate the preference of the interaction between Mn²⁺ and polysulfides. The as-prepared MnO₂-coated sulfur cathodes showed an excellent long-term cycling over 1500 cycles with over 71.7% capacity retention, indicating the promising practical application in future.

2.1.5. Hollow Structured Coating Materials

As previously mentioned, various materials such as polymer, graphene, and metal oxides have been developed as coatings for sulfur composites. However, the volume expansion of sulfur cathodes was found to be a challenge for coating materials as it may shorten the service life of the coating layer and directly hinder the performance of the cathodes. To address this challenge, novel nanostructures of coating materials have been designed to accommodate the volume expansion of sulfur composites.

Cui and co-workers first calculated the volume expansion of sulfur cathodes and also raised the idea of maintaining space between the sulfur cathode and coating structure, as shown in Figure 2j.^[32] During synthesis, TiO₂ was employed as a coating material on sulfur particles, and a portion of sulfur was then removed to form an internal void space. The obtained

yolk-shell structure has enough space to accommodate the volume expansion of sulfur cathodes and minimizes the dissolution of polysulfides into electrolyte. As a result, the yolk-shell sulfur-TiO₂ composites used as cathodes demonstrate stabilized performance during cycling with a capacity decay as small as 0.033% per cycle over 1000 charge/discharge cycles. Following this idea, other yolk-shell structure sulfur composites were also reported by using conductive carbon-based coating materials, further demonstrating this concept with improved electrochemical performance of Li-S batteries.^[45] Although the yolk-shell coating structure provides protection for sulfur cathodes, such structure still requires elaborate synthetic procedures involving controlled TiO₂ coating and precise chemical etching to dissolve a specific amount of sulfur to generate the internal void space. Furthermore, the electronic and ionic conductivities of TiO₂ are limited for sulfur cathodes. In response to these issues, Cui and co-workers developed a polyvinyl pyrrolidone-sulfur (PVP-S) composite with an O-ring structure, as shown in Figure 2k.^[33] During the lithiation process, the PVP coating layer forces sulfur to expand toward the center of the O-ring void space to avoid the dissolution of polysulfides. The electrochemical performance shows improved cycling stability over 1000 cycles with a capacity decay as low as ≈0.46 mAh g⁻¹ per cycle, demonstrating the promising design of O-ring coating structures for sulfur cathodes.

In brief, various coating materials have been developed for sulfur and Li₂S-based composites in Li-S batteries, such as polymer, graphene, CVD carbon, and metal oxides, as summarized in Table 1. Conductive carbon materials are attractive coating materials for sulfur and Li₂S-based composites. For sulfur-based composites, the synthesis of coating materials is mainly solution-based chemical methods. For Li₂S-based composites, due to their air and moisture sensitivity, CVD and high-temperature carbonization under inert atmosphere are preferred strategies for coating synthesis. Most carbon coating materials have been demonstrated to improve the conductivity of cathodes and reduce the dissolution of polysulfides. Both the coated sulfur and Li₂S cathodes present stabilized cycle life with increased capacity in Li-S batteries. Yolk-shell and O-ring structures are attractive interface designs for sulfur composites that can accommodate volume expansions during the lithiation process, demonstrating novel nanostructure design to address specific challenges for sulfur cathodes. The electrochemical results illustrate the robustness of coating structure during discharge-charge processes and the highly stabilized cycle life of sulfur cathodes in Li-S batteries. However, most reported sulfur/Li₂S composites have low sulfur loading in electrodes, as summarized in Table 1. In addition to nanostructure design, sulfur loading and electrolyte/sulfur ratio are also very important factors in the development of high-energy Li-S batteries. High-loading sulfur cathodes with these novel nanostructure composites should be further developed for high-energy Li-S batteries.

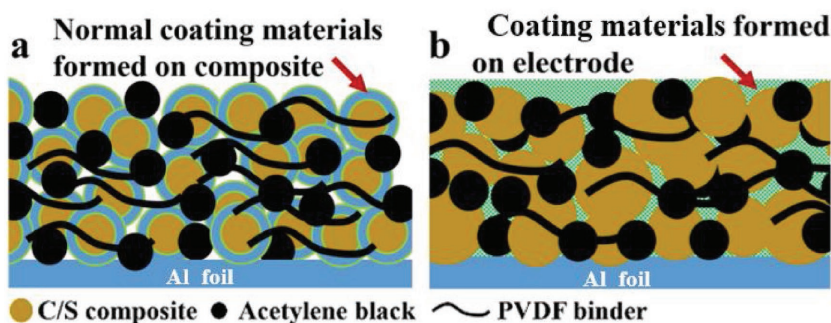


Figure 3. Comparison of coating materials a) on composites and b) on electrodes. a,b) Reproduced with permission.^[13] Copyright 2016, American Chemical Society.

2.2. Development of Coating Materials for Sulfur-Based Electrodes

In addition to directly coating on sulfur-based composites, an alternative interface design is to place the coating or interlayer directly on the formed electrodes. Compared with traditional coating materials formed on composites, this strategy facilitates the preservation of the electrode conductive network, as shown in Figure 3. In this case, the synthesis of such coatings or interlayers on electrodes cannot use the traditional solution-based strategies, and mostly employs a slurry method or other advanced synthetic procedures. The purpose of the coating or interlayer is to slow down the diffusion of dissolved polysulfides into the electrolyte and act as a reservoir to re-utilize these species in electrochemical reactions. Until now, various materials such as polymer, graphene, and carbon-metal oxide composites have been developed as coating materials on electrodes.

2.2.1. Carbon-Based Coating Materials on Sulfur-Based Electrodes

Conductive and lightweight carbon materials are attractive coating materials and interlayers for sulfur-based electrodes. Huang and co-workers reported a lightweight TiO₂/graphene thin film as an interlayer deposited on sulfur-based electrodes via a simply slurry method, as shown in Figure 4a.^[46] The author proposed that the porous graphene affords an additional electronically conductive network and can physically trap sulfur and polysulfides, while the TiO₂ in the graphene/TiO₂ barrier film can further chemically suppress the dissolution of polysulfides to alleviate the undesirable shuttle effect. The typical electrolyte color test and UV-vis absorption analysis of the cycled electrodes further demonstrated the TiO₂/graphene thin film suppress the diffusion of polysulfide species. The sulfur cathodes coated by the graphene/TiO₂ film deliver a reversible specific capacity of 1040 mA h g⁻¹ over 300 cycles at 0.5 C. Afterward, Wang and co-workers reported an ultrathin dendrimer-graphene oxide composite film via a similar slurry casting method, as shown in Figure 4b.^[47] The dendrimer molecules provide a strong affinity to polysulfides via chemical interactions between amide groups and Li ions, while the graphene oxide film ensures mechanical robustness and a low thickness of 100 nm. In addition to the slurry method, Yang and co-workers employed an electrostatic-spraying approach to

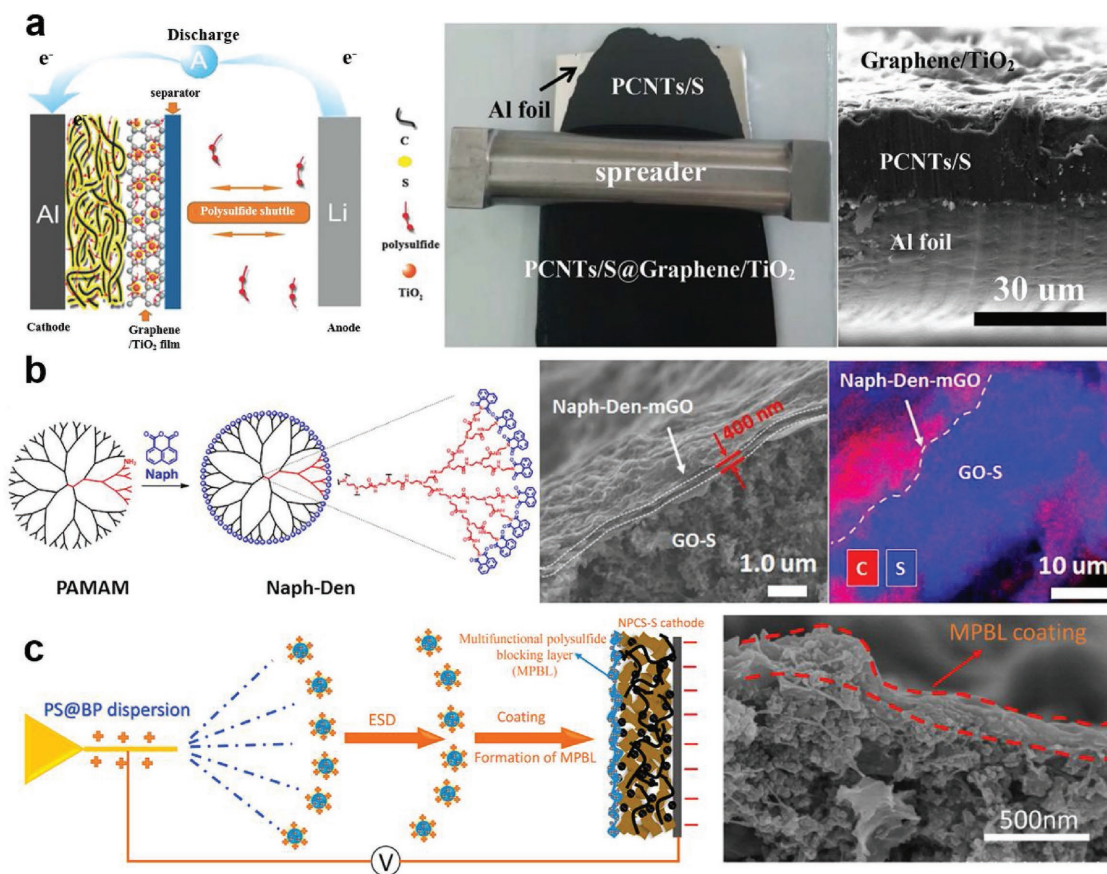


Figure 4. Various carbon materials deposited on electrodes. a) Graphene/TiO₂ interlayer. Reproduced with permission.^[46] Copyright 2015, John Wiley & Sons, Inc. b) Polymer–graphene oxide thin-film interlayer. Reproduced with permission.^[47] Copyright 2017, National Academy of Sciences. c) Electrostatic spray deposited PEDOT:PSS coating. Reproduced with permission.^[48] Copyright 2016, Elsevier.

develop ultrathin and compact coatings onto sulfur electrodes, as shown in Figure 4c.^[48] Commercial carbon powder BP2000 and conductive polymer PEDOT:PSS are used in the precursor dispersion in the electrostatic-spraying process. The conductive carbon and polymer thin film (100 nm) guarantee fast ion diffusion, and the robust structure helps block polysulfides with physical and chemical absorption. Thus, the as-prepared sulfur cathode exhibits a good cycling performance with only 0.042% capacity decay per cycle at 1 C for 1000 cycles. Compared to complicated synthetic methods of traditional coating materials, these coating approaches are very easy to achieve and can be extended to various sulfur-based electrodes, providing the possibility for large-scale application.^[49] It should be noted that it is difficult to precisely control the uniformity and thickness using these methods. With the introduced carbon-based coatings and interlayers, the energy density of the batteries will thereby be reduced to some extent.

2.2.2. Atomic and Molecular Layer Deposited Coating Materials

Atomic and molecular layer deposited (ALD and MLD) coating materials are novel ultrathin film gas-phase deposition techniques.^[50,52] They consist of self-limiting binary reactions and demonstrate unparalleled advantages in producing uniform

and conformal thin films, providing precise control over film thickness and chemical composition of the target material at an atomic and/or molecular scale, as shown in Figure 5a.^[53] Until now, ALD and MLD techniques have been used to develop many kinds of thin-film materials such as metal oxides, nitrides, sulfides, polymers, and hybrid inorganic–organic films.^[54] Different from traditional coating materials, ALD and MLD coatings are deposited directly on the electrode and are proposed to preserve the conductive network within the electrode. Furthermore, the ultrathin and controllable ALD/MLD films are beneficial for Li-ion diffusion into sulfur cathodes, while the uniformity of the ALD/MLD coating localizes sulfur active materials to prevent dissolution.^[50,53b] In addition, the low-temperature operation of ALD and MLD processes maintains the properties of sulfur electrodes to a large extent.^[54b,55] Therefore, ALD and MLD thin-film materials are promising coating materials for sulfur electrodes. As shown in Figure 5b, Yushin and co-workers first reported the use of plasma-enhanced ALD (PEALD) to coat sulfur cathodes with Al₂O₃.^[51] The Al₂O₃-coated sulfur–carbon fiber composites show uniform morphology after cycling and retain a high sulfur loading within the electrode. Furthermore, the lithium metal anode displays a smooth surface morphology in conjunction with the PEALD-coated sulfur cathode, indicating that the dissolution of sulfur into the electrolyte was greatly reduced with the

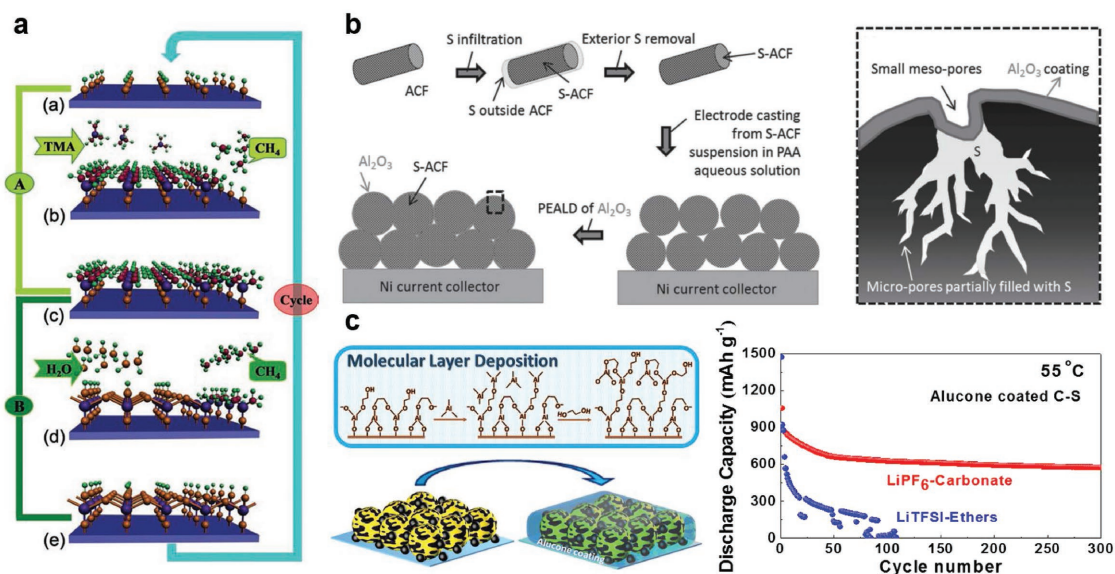


Figure 5. ALD and MLD coating materials applied to sulfur electrodes. a) Schematic figure of a typical ALD process. Reproduced with permission.^[50] Copyright 2012, John Wiley & Sons, Inc. b) Plasma-enhanced ALD Al_2O_3 coating for sulfur cathodes. Reproduced with permission.^[51] Copyright 2013, John Wiley & Sons, Inc. c) MLD alucone coating for safe high-temperature Li-S batteries. Reproduced with permission.^[13] Copyright 2016, American Chemical Society.

protection of the PEALD coating. Following this report, other research groups have also reported the use of ALD Al_2O_3 coating for various C-S electrodes.^[56] It has been found that the ALD Al_2O_3 thin film is a simple and effective coating in preventing sulfur dissolution. Additionally, the ALD Al_2O_3 partially evolves into AlF_3 and LiAlO_2 during electrochemical processes, resulting in a solid-state electrolyte that improves Li-ion transport kinetics in the sulfur cathodes.^[56a] With the development of MLD materials, Sun and co-workers first employed an alucone thin film via MLD as a protective coating for sulfur cathodes.^[57] The growth mechanism of MLD thin films is similar to that of ALD films,^[58,59] but rather than using water as a precursor during the oxidation pulse, MLD introduces organic precursors which allow for the production of polymer and polymer-metal hybrid thin films. Taking ALD Al_2O_3 and MLD alucone for instance, H_2O is used to form the ALD Al_2O_3 while ethylene glycol (EG) is the analogous precursor used to synthesize alucone thin films via MLD. Due to the introduction of carbon-containing precursors, MLD alucone has demonstrated porous structure and reinforced mechanical properties. Compared to ALD Al_2O_3 -coated C-S electrodes, the MLD alucone-coated C-S electrodes present improved cycling stability and prolonged cycle life, indicating that MLD techniques are a promising approach for the development of coatings for sulfur cathodes and other energy storage systems.^[57]

In addition to its role as a physical protecting layer for sulfur cathodes, ALD and MLD ultrathin coating materials are notable for enabling new electrochemical reactions to address crucial challenges of Li-S batteries. With the application of an MLD alucone coating, Sun and co-workers developed a safe and durable high-temperature Li-S battery, as shown in Figure 5c.^[13] A major drawback of the popular ether-based Li-S electrolyte is the relatively low boiling and flash point, raising plenty of safety concerns for the use of Li-S batteries

at high temperatures.^[59b] Compared to ether-based electrolytes, carbonate-based electrolytes have been proven to be stable and widely accepted for use in high-temperature Li-ion batteries.^[60] However, carbonate-based electrolytes applied to Li-S batteries were rarely successful due to the side reactions between sulfur species and carbonate solvents. With the use of synchrotron-based X-ray near-edge absorption spectroscopy (XANES), Sun and co-workers found that the alucone MLD coating prevents the direct contact of carbonate electrolyte and sulfur but still allows Li-ion transport. The MLD alucone-coated C-S electrode demonstrates stable and prolonged cycle life at high temperatures. Although the research demonstrated improved performance of Li-S at high temperatures, the cycle capacity and Coulombic efficiency of alucone-coated C-S electrodes at room temperature still need improvement and may be related to inefficient use of the Li anode, thus requiring further optimization of the carbonate-based electrolyte system.^[13]

In this section, we summarized the interface design and the developed coating materials for sulfur cathodes in Li-S batteries. In the past decades, various coating materials have been reported for sulfur and Li_2S cathode materials, including conductive polymers, graphene, amorphous carbon, and metal oxides. These coating materials generally have mild synthetic procedures that are easily obtainable in most laboratory conditions with minimal economic cost. Most of the reported coating materials for sulfur-based composites are designed to prevent polysulfide dissolution and improve conductivity of cathodic active materials. The reported novel hollow structured coating materials enable sulfur cathodes to accommodate the volume expansion during the lithiation process, which emphasize the significance of the interface design on sulfur cathodes. On the other hand, using coatings directly deposited on electrodes is another attractive strategy for sulfur-based cathodes. In particular, ALD and MLD techniques are novel interface strategies

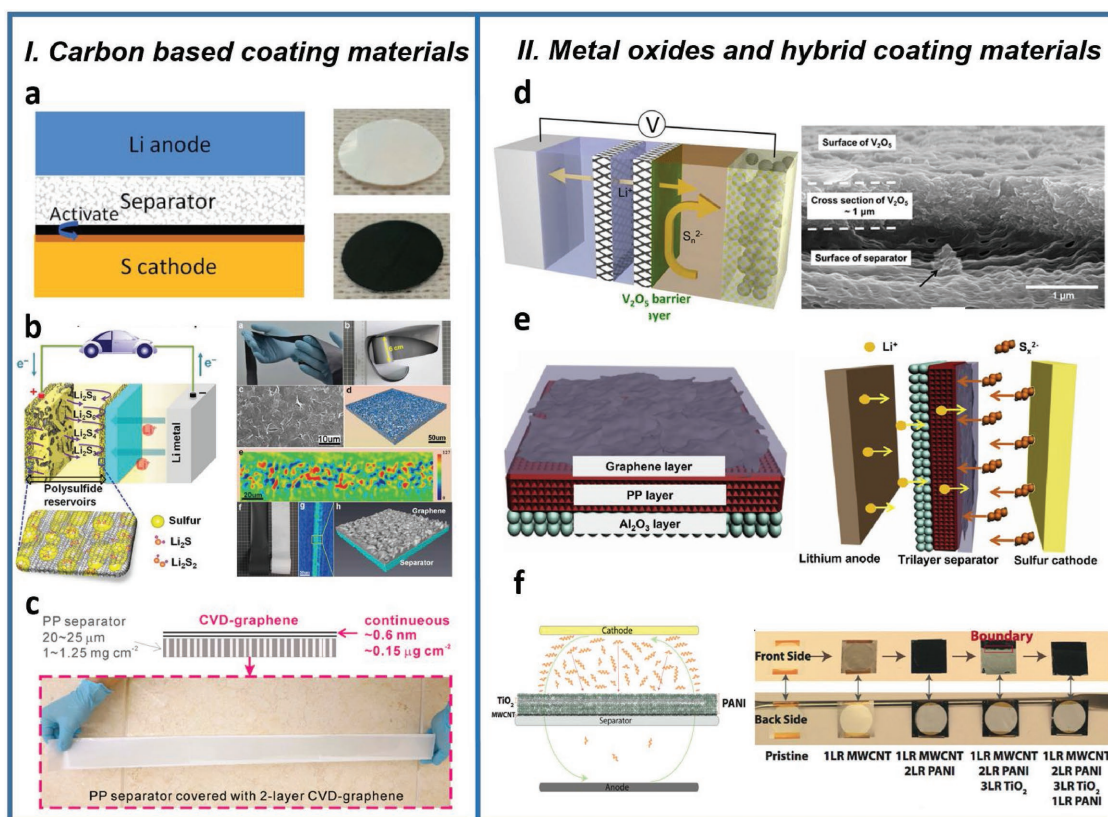


Figure 6. Various coating materials applied to separators in Li-S batteries. I. Carbon-based coating materials: a) Commercial porous carbon coating Super P. Reproduced with permission.^[14] Copyright 2014, Royal Society of Chemistry. b) Graphene-coated separator. Reproduced with permission.^[71] Copyright 2014, John Wiley & Sons, Inc. c) CVD-graphene. Reproduced with permission.^[72] Copyright 2017, American Chemical Society. II. Metal oxides and hybrid coating materials: d) V₂O₅ barrier layer. Reproduced with permission.^[73] Copyright 2014, American Chemical Society. e) Trilayer separator with graphene and Al₂O₃ coating. Reproduced with permission.^[74] Copyright 2016, Elsevier. f) MWCNT-PANI-TiO₂. Reproduced with permission.^[75]

to deposit ultrathin film coating for sulfur cathodes with precise control over thickness and composition. The ALD/MLD thin-film coating materials, including metal oxides, multielement metal oxides, and metal-organic hybrid composites, can be tailored and designed according to their applications. Furthermore, ALD and MLD techniques enable conformal thin films to be deposited directly on electrodes, which is difficult to achieve using other coating strategies. Although the conductivity of state-of-the-art ALD and MLD thin films still needs to be further improved, they are proposed to be a promising coating technology for Li-S batteries and other energy storage systems.

3. Interface Design on Separators in Li-S Batteries

Coating and interlayer materials applied to separators in Li-S batteries are primarily to prevent the shuttling of dissolved polysulfides between the anode and cathode, as shown in Figure 1d.^[14,70] The modified separators in Li-S batteries are supposed to have following characteristics: 1) chemical and/or physical sorption to trap dissolved polysulfides, 2) enough space as a reservoir to maintain polysulfides, and 3) good electronic conductive path to reutilize the adsorbed/bonded polysulfides in electrochemical reactions. Following these features, various

separators with coating materials and freestanding interlayers have been developed in Li-S batteries.

3.1. Development of Coating Materials on Separators in Li-S Batteries

Carbon materials such as conductive carbon powder, graphene, and polymers are favorable as coating materials for separators to prevent the migration of polysulfides and the accumulation of the inactive S-related species layer at the anode.^[76] The coating deposition process is mostly carried out via the slurry casting method. Cui and co-workers developed a conductive carbon coating on a separator using commercial carbon Super P, as shown in Figure 6a.^[14] The electrochemical performance demonstrates a significantly improved cycling stability of the Li-S battery with the use of a coated separator compared with pristine one. Cheng and co-workers reported the use of a graphene-coated separator to serve as a reservoir for dissolved polysulfides, as shown in Figure 6b.^[77] As claimed in literature, the low weight of graphene is favorable for maintaining high energy densities as well as enabling large-scale production for graphene-coated separators. It should be highlighted that the paper first time employed 3D X-ray microtomography (XRM) to investigate the sulfur diffusion evolution in the electrode

during cycling. As shown from the scanning electron microscopy (SEM), TEM, and XRM results, sulfur is captured by graphene nanosheets in a homogeneous state and the as-prepared graphene separator provides effective contact between the sulfur and the separator, and functions as an embedded conductive network that enables fast electron and lithium-ion transport.

Many other carbon-based materials are also employed as coating materials applied to separators in Li–S batteries, such as porous carbon, carbon nanotubes, surface-modified carbon nanotubes, and graphene oxides.^[14,70a,b,71,76,78] Manthiram and co-workers have recently developed a boron-doped carbon nanotube (B-CNT)-coated separator in Li–S batteries.^[79] The paper carried out an interesting polysulfides diffusion test to demonstrate the excellent polysulfide-trapping ability of B-CNTs with their polarized surface. Many other MWCNTs and MWCNTs–polymer coating materials have also been reported by Manthiram and co-workers.^[78a,80] Kim et al. reported another functional CNT-coated separator in Li–S batteries. The paper emphasized that the hydroxyl groups from CNTOH provoke strong interaction with lithium polysulfides and result in effective trapping of lithium polysulfides.^[81] Interestingly, the paper calculated the theoretical bonding energies of lithium polysulfides (Li_2S_x , $x = 1-8$) with bare CNTs and functional CNTOHs. Compared with bare CNTs, the higher bonding energy of CNTOH with Li_2S_x well demonstrates the strong trapping ability of functionalized CNTOH to polysulfides, indicating the excellent electrochemical performance with the use of a modified separator. It should be noted that the employed slurry casting method does not allow for precisely controlled thin-layer coatings, resulting in micrometer-scale thicknesses for most of the aforementioned carbon coatings. Furthermore, binder additives are inevitable in most slurry preparations to combine the individual carbon materials, which increase the inactive components in batteries. To overcome the aforementioned challenges from the slurry casting method, Wan and co-workers developed a CVD-grown graphene film on a separator with control of the coating thickness down to the atomic level, as shown in Figure 6c.^[72] Unlike the coating materials via slurry casting which consist of discrete nano/microstructures with microscale thickness, the thickness of the CVD–graphene is ≈ 0.6 nm with an areal density of $0.15 \mu\text{g cm}^{-2}$, which is negligible in relation to the dimensions of a commercial polypropylene (PP) separator. The CVD–graphene on a PP separator demonstrates the thinnest and lightest interlayer to date and is able to suppress the shuttling of polysulfides during cycling, leading to improved electrochemical performance and suppressed self-discharge in developed Li–S batteries.

In addition to pure carbon-based coatings on separators, metal oxide and metal oxide–carbon hybrid coatings have also been developed for Li–S batteries. Liu and co-workers describe a micrometer-scale V_2O_5 metal oxide barrier on a separator for Li–S batteries via a spin-coating method.^[73] As shown in Figure 6d, this layer stops the diffusion of dissolved polysulfide anions between the sulfur cathode and the Li anode while permitting solid-state transport of Li^+ cations. Li and co-workers proposed a metal oxide–carbon hybrid coating using trilayered graphene/polypropylene/ Al_2O_3 as a separator for Li–S batteries.^[74] As shown in Figure 6e, graphene is coated on one side of a PP separator as a conductive layer and a reservoir for rapid electron–ion

transport and polysulfide reservation. The Al_2O_3 particles are coated on the other side to further enhance thermal stability and safety of the separator facing the Li anode. Many other metal oxide–carbon hybrid coatings, such as $\text{Li}_4\text{Ti}_5\text{O}_{12}$ –graphene, TiO_2 –carbon black, Al_2O_3 –CNTs, are also reported as coating materials applied to separators to stop the diffusion of polysulfide anions between the sulfur cathode and Li anode.^[82]

Except for exploring novel materials, facile coating approaches are attractive studies in the design of separators. Archer and co-workers employed a Langmuir–Blodgett–Scooping (LBS) technique to fabricate a PANI– TiO_2 –MWCNTs coating on a separator, as shown in Figure 6f.^[75] The LBS method not only takes advantage of self-assembly and Marangoni stresses at an air/water interface without the need of binders, but also holds for large-scale industrial deployment. The developed PANI– TiO_2 –MWCNT coating demonstrates excellent performance in Li–S batteries, and the LBS method has also been employed to develop various carbon–metal oxides’ coatings for separator interface modification.^[83]

3.2. Development of Freestanding Interlayers for Separators in Li–S Batteries

Besides modifying separators with coating materials, an alternative promising strategy is to insert a freestanding interlayer as a part of the separator. The interlayer should allow smooth Li-ion diffusion and at the same time trap or block polysulfides at the cathode. Manthiram and co-workers developed various freestanding interlayers with different carbon-based materials in Li–S batteries.^[15,84,85,87] As shown in Figure 7a, they first developed a microporous carbon paper as an interlayer in Li–S batteries.^[15] With a bifunctional microporous carbon paper between the cathode and the separator, a significant improvement was observed in both the active material utilization and capacity retention. The insertion of a microporous carbon interlayer decreases the internal charge transfer resistance and localizes the soluble polysulfide species, demonstrating the commercially feasible value of Li–S batteries in application. In addition to microporous carbon interlayers, Manthiram and co-workers have also developed various interlayer materials such as carbon nanofibers, multiwalled carbon nanotubes, graphene, nitrogen-doped graphene, biomass-derived carbon papers, and carbonized newspaper for applications in Li–S batteries (Figure 7b,c).^[84,85,87] As mentioned in the literature, the reported freestanding carbon-based interlayers always possess hierarchically porous structure and a 3D interwoven network for absorbing/trapping the active material, channeling the electrolyte, and transporting electrons.

In addition to pure carbon freestanding interlayers, multi-composites and hybrid freestanding interlayers have also been reported in many studies. As shown in Figure 7d, Yin and co-workers described a flexible freestanding ternary NiO/reduced graphene oxide (RGO)-Sn hybrid film in Li–S batteries.^[61] The developed freestanding interlayer is inserted between the sulfur cathode and separator to trap sulfur species and polysulfides. The authors claim that NiO, with its porous structure, facilitates polysulfide storage, while the flexible RGO accommodates the volume change of sulfur cathodes, which improve

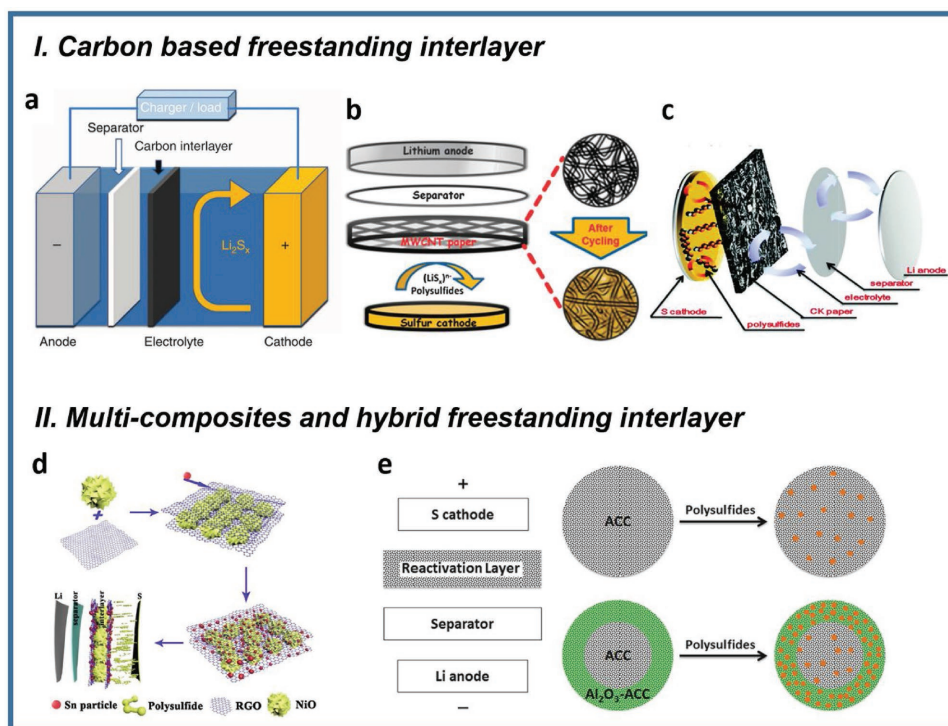


Figure 7. Various freestanding carbon-based interlayer materials applied to Li-S batteries. a–c) Carbon-based freestanding interlayers. a) Reproduced with permission.^[15] Copyright 2012, Nature Publishing Group. b) Reproduced with permission.^[84] Copyright 2014, Royal Society of Chemistry. c) Reproduced with permission.^[85] Copyright 2015, Royal Society of Chemistry. d,e) Multicomposites and hybrid freestanding interlayers. d) Reproduced with permission.^[61] Copyright 2017, Elsevier. e) Reproduced with permission.^[86] Copyright 2013, Elsevier.

the electrochemical performance. Various hybrid freestanding interlayers have also been attempted in Li-S batteries, such as nano-TiO₂-decorated carbon nanofiber, CoS₂/carbon paper, and V₂O₅-decorated carbon nanofibers.^[25,88] Most of the employed metal oxides and sulfides are ascribed to localize polysulfides. Therefore, precise control of the thickness and uniformity of these oxides/sulfides on substrates is crucial to the battery performance. ALD thin-film techniques are attractive coating strategies to achieve atomic level thickness of metal oxides on freestanding interlayers. Hu and co-workers reported ALD Al₂O₃-coated carbon cloth as part of the separator used in Li-S batteries, as shown in Figure 7e.^[86] Compared with bare carbon cloth, the ALD Al₂O₃-coated carbon interlayer facilitates the sorption of polysulfides from the cathode and increases the utilization of dissolved sulfur during electrochemical reactions, effectively relieving the “shuttle effect” in Li-S batteries.

In summary, the interface at the separator of Li-S batteries is mostly designed to prevent the migration of polysulfides. The reported coating and interlayer materials for separators have successfully diminished the accumulation of dissolved polysulfides, and facilitate the reactivation of dissolved polysulfides in the electrochemical processes within the battery. The Li-S batteries with coated separators and freestanding interlayers thereby demonstrate improved capacities as well as stabilized cycle lives. However, there are still challenges in the development of coated separators in Li-S batteries. First, it is notable that the capacity calculation of Li-S batteries in most of reported literature is only based on sulfur active materials or sulfur cathodes. The decrease of the total capacity and energy

density with the introduction of coating materials and freestanding interlayers is not considered. Second, the consumption of electrolyte with the added carbon materials will increase and therefore decrease the energy density of batteries. As summarized in Table 2, many studies investigated the performance of high-loading sulfur cathodes with a coated separator or freestanding interlayers. However, very few mentioned the mass of electrolyte added to the batteries, which should be investigated in detail for future research. Third, most of the modified separators and freestanding interlayers are designed to overcome the challenges of sulfur cathodes, but a few focus on the protection of the lithium metal anode. Thereby, multifunctional separators or freestanding interlayers for both sulfur cathodes and Li metal anodes are promising directions for future interlayer designs.

4. Interface Design and Coating Materials for Lithium Anode Protection

Most state-of-the-art Li-S batteries employ lithium metal as anodes. Although lithium metal anodes have a high energy density, it suffers from a number of challenges when facing practical application.^[103] First, lithium metal easily reacts with surrounding electrolyte solvents and dissolved polysulfides, as shown in Figure 8.^[104] The reacted lithium metal and decomposed electrolyte will form an insulated SEI layer which increases the resistance of batteries and significantly hinders the transportation of Li ions, resulting in low Coulombic

Table 2. Summary of modified separators and freestanding interlayers for Li–S batteries.

Name		Mass load	Thickness of coating	Sulfur load	Sulfur content [wt%]	Performance	Ref.	
Coated separator	Carbon-based coating materials	Polyvinylidene Fluoride (PVDF)-carbon thin film	0.068 mg cm ⁻²	Not mentioned	7 mg cm ⁻²	70	669 mAh g ⁻¹ (0.5 C, 500 cycles)	[70b]
		Graphene thin film	1.3 mg cm ⁻²	20 μm	2.1–2.8 mg cm ⁻²	70	1000 mAh g ⁻¹ (0.46 C, 100 cycles)	[71]
		A porous N, P dual doped graphene	1.0 mg cm ⁻² (total 3.0 mg cm ⁻²)	Not mentioned	Not mentioned	70	638 mAh g ⁻¹ (1 C, 500 cycles)	[89]
		Carbon nanotube-coated separator	0.14 mg cm ⁻² Totally 1.34 mg cm ⁻²	8.4 μm	3 mg cm ⁻²	70	570 mAh g ⁻¹ (0.5 C, 400 cycles)	[90]
		B-RGO coating	0.2–0.3 mg cm ⁻²	25 μm	1.5 mg cm ⁻²	56	593 mAh g ⁻¹ (2 C, 100 cycles)	[91]
		Polypropylene/graphene/Nafion	GO 0.0032 mg cm ⁻² Nafion 0.05 mg cm ⁻²	GO 30 nm Nafion 100 nm	1.2–4.0 mg cm ⁻²	54	700 mAh g ⁻¹ (0.5 C, 200 cycles)	[92]
		Porous graphene-modified separator	0.54 mg cm ⁻²	10 μm	1.8–2.0 mg cm ⁻² 7.8 mg cm ⁻²	63	877 mAh g ⁻¹ (0.5 C, 150 cycles)	[93]
		CVD graphene film on separator	CVD-G 0.15 μg cm ⁻² Total 1.34 mg cm ⁻²	CVD-G 0.6 nm Total 25 μm	1 mg cm ⁻²	70	600 mAh g ⁻¹ (0.5 C, 1500 cycles)	[72]
		g-C ₃ N ₄ -coated separator	1.5 mg cm ⁻²	26 μm	1.7 mg cm ⁻² 5 mg cm ⁻²	54	840 mAh g ⁻¹ (0.5 C, 400 cycles) 901.6 mAh g ⁻¹ (0.1 C, 40 cycles)	[94]
		Carbon–metal oxides hybrid coating	V ₂ O ₅ barrier layer	Not mentioned	1 μm	1.25 mg cm ⁻²	61.8	800 mAh g ⁻¹ (C/15, 250 cycles)
	CNTs/Al ₂ O ₃ /PP trilayer		Not mentioned	Al ₂ O ₃ 5 μm CNT 12 μm	0.42 mg cm ⁻²	42	800 mAh g ⁻¹ (0.2 C, 100 cycles)	[82a]
	LBS MWCNT/PANI/TiO ₂		TiO ₂ 40 μg cm ⁻² MWCNT 5 μg cm ⁻² PANI 100 μg cm ⁻²	TiO ₂ 300 nm MWCNT 80 nm PANI 3 μm	1.2 mg cm ⁻² 3.5 mg cm ⁻²	43 63	1090 mAh g ⁻¹ 780 mAh g ⁻¹ (0.5 C, 250 cycles)	[75]
	LBS MWCNT/SiO ₂ /MWCNT		130 mg cm ⁻²	3 μm	1.1 mg cm ⁻² 5 mg cm ⁻²	50 70	1000 mAh g ⁻¹ (0.5 C, 250 cycles)	[83]
	Graphene/PP/Al ₂ O ₃		Graphene 0.1 mg cm ⁻² Al ₂ O ₃ 1.22 mg cm ⁻²	Graphene 3–5 μm Al ₂ O ₃ 5 μm	0.75 mg cm ⁻²	60	800 mAh g ⁻¹ (0.2 C, 100 cycles)	[74]
	Li ₄ Ti ₅ O ₁₂ /graphene coating		0.346 mg cm ⁻²	30 μm	1.0–1.2 mg cm ⁻²	60	793 mAh g ⁻¹ (0.3 C, 300 cycles)	[82b]
	Nano TiO ₂ /carbon black		0.7 mg cm ⁻²	7.5 μm	2 mg cm ⁻²	60	501 mAh g ⁻¹ (0.5 C, 500 cycles)	[82d]
	Ketjen Black (KB) carbon/Ir-modified separator		0.2 mg cm ⁻²	20 μm	0.8 mg cm ⁻²	60	689 mAh g ⁻¹ (0.2 C, 100 cycles)	[95]
	Nano TiO ₂ -decorated carbon coating		0.2 mg cm ⁻²	4 μm	2.0 mg cm ⁻²	63	800 mAh g ⁻¹ (0.5 C, 200 cycles)	[82c]
	Free-standing interlayer	Carbon-based free-standing interlayer	Bifunctional microporous carbon interlayer	Not mentioned	Not mentioned	Not mentioned	70	1000 mAh g ⁻¹ (1 C, 100 cycles)
Hierarchical carbonized paper			0.23 mg cm ⁻² *6	35 μm×6	1.1 mg cm ⁻²	60	1192 mAh g ⁻¹ (1 C, 100 cycles)	[84]
Freestanding carbon nanofiber interlayer			4.2 mg cm ⁻²	280 μm	1.4 mg cm ⁻²	60–70	>1200 mAh g ⁻¹ (C/5, 100 cycles)	[85]
Electroactive cellulose–graphene oxide interlayer			0.5 mg cm ⁻²	Not mentioned	0.6 mg cm ⁻²	48	474 mAh g ⁻¹ (0.2 C, 200 cycles)	[96]
N-doped 3D porous graphene			1.29 mg cm ⁻² (R = 0.7 cm)	Not mentioned	Not mentioned	70	780 mAh g ⁻¹ (0.1 C, 100 cycles)	[97]

Table 2. Continued.

Name	Mass load	Thickness of coating	Sulfur load	Sulfur content [wt%]	Performance	Ref.	
Cyclized-polyacrylonitrile- carbon nanofiber (CP@CNF) film	0.8–1.2 mg cm ⁻²	30 μm	1.2 mg cm ⁻²	60	910 mAh g ⁻¹ (0.3 C, 100 cycles)	[98]	
N-doped conductive interlayer	2 mg cm ⁻²	Not mentioned	3 mg cm ⁻²	75	613 mAh g ⁻¹ (0.1 C, 200 cycles)	[99]	
Web-structured graphitic carbon fiber felt	Not mentioned	56 μm	0.7 mg cm ⁻²	60	830 mAh g ⁻¹ (1 C, 300 cycles)	[100]	
Reduced graphene oxide/activated carbon interlayer	3.5 mg cm ⁻²	0.21 mm	4 mg cm ⁻²	46.4	655 mAh g ⁻¹ (0.1 C, 100 cycles)	[101]	
Carbon nanofiber interlayer	1.53 mg cm ⁻²	80 μm	1.5 mg cm ⁻²	70	917 mAh g ⁻¹ (0.2 C, 200 cycles)	[102]	
Hybrid carbon-based freestanding interlayer	ALD Al ₂ O ₃ -coated carbon cloth	10 mg cm ⁻²	0.5 mm	12 mg cm ⁻²	59	766 mAh g ⁻¹ (40 mA g ⁻¹ , 40 cycles)	[86]
	TiO ₂ -decorated carbon nanofiber	0.5–0.6 mg cm ⁻²	35 μm	0.8 mg cm ⁻²	60	694 mAh g ⁻¹ (1 C, 500 cycles)	[88b]
	Porous CoS ₂ /carbon paper	Not mentioned	0.3 mm	0.97–1.3 mg cm ⁻²	64	818 mAh g ⁻¹ (0.1 C, 200 cycles)	[88a]
	Ternary NiO/RGO-Sn flexible freestanding film	1.4 mg cm ⁻²	3.5–9.0 μm	4 mg cm ⁻²	80	868 mAh g ⁻¹ (100 mA g ⁻¹ , 150 cycles)	[61]
	V ₂ O ₅ -decorated carbon nanofiber	1 mg cm ⁻²	Not mentioned	2 mg cm ⁻²	70	567 mAh g ⁻¹ (3 C, 1000 cycles)	[25]

efficiency and diminished cycle life of Li–S batteries.^[103a] Additionally, the dissolved polysulfides in Li–S batteries eventually migrate toward the lithium metal, which inevitably corrodes the lithium metal forming insoluble Li₂S/Li₂S₂ products on the Li anode surface.^[105] Furthermore, prevention of lithium dendrite formation is crucial safety risk for Li–S batteries.^[5,103a] As reported in literature, one advantage of Li–S batteries is the dendrite-free growth of lithium resulting from the reaction between the dissolved polysulfides in ether-based electrolytes and the lithium metal surface, which suppresses lithium dendrite formation within Li–S batteries.^[104] However, Li–S batteries containing high-loading sulfur

cathodes or operating at high current densities may form lithium dendrites rapidly, which poses significant safety risks in battery operation. Therefore, development of safe and high-energy Li-metal is essential for high-energy Li–S batteries. An ideal protection layer for Li anodes is a thin-film coating with the following properties: 1) conformality to avoid the side reactions with solvents and polysulfides; 2) good ionic conductivity to allow fast Li-ion transportation; and 3) a facile synthesis that can be performed in the absence of air and moisture. Based on the aforementioned requirements, we generally classify the coating and interlayer materials in terms of their synthetic procedure: i) preformed

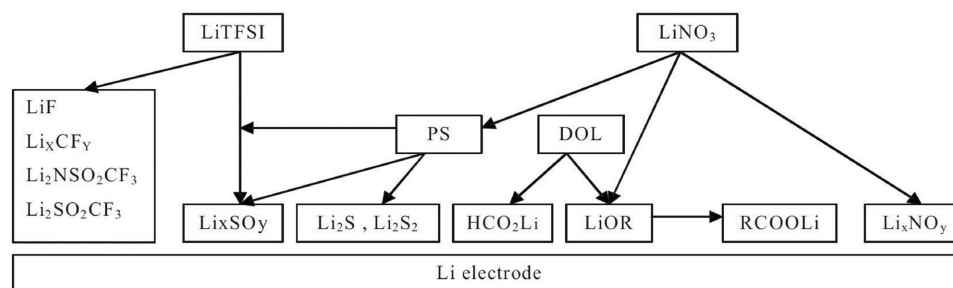


Figure 8. Schematic illustration of the various components in typical Li–S ether-based electrolyte to the surface chemistry on the Li metal anode. Reproduced with permission.^[106] Copyright 2009, The Electrochemical Society.

Table 3. Summary of reported thin-film coating materials on Li anodes applied in Li–S batteries.

Name	Thickness of coating	Sulfur loading	Sulfur content [wt%]	Performance	Ref.	
Preformed artificial coating materials	Poly(ethylene glycol)-coated Li foil (UV curing)	10 μm	2.0 mg cm^{-2}	50	270 mAh g^{-1} (100 cycles, N/A)	[109]
	Polypyrrole coating on Li powder	2 μm	N/A	60	500 mAh g^{-1} (0.1 C, 50 cycles)	[110a]
	PEDOT-co-PEG-coated Li foil	10 μm	2.5–3 mg cm^{-2}	56	815 mAh g^{-1} (0.5 C, 300 cycles)	[110b]
	Li_3N -coated Li foil	200–300 nm	2.5–3 mg cm^{-2}	56	773 mAh g^{-1} (500 cycles, 0.5 C)	[107]
	Al_2O_3 -coated Li foil	1.7–3.7 μm	1.1–1.6 mg cm^{-2}	49	850 mAh g^{-1} (50 cycles, 0.1 C)	[111]
	ALD Al_2O_3 -coated Li foil	14 nm	5 mg cm^{-2}	N/A	>1000 mAh g^{-1} (100 cycles, 0.14 mA cm^{-2})	[16]
	Carbon paper interlayer on Li foil	210 μm (mono, 1–5 layers)	2.8–3.0 mg cm^{-2}	56	600 mAh g^{-1} (150 cycles, 0.1 C)	[108]
In situ formed coating materials	LiODFB electrolyte additive supported Li foil	N/A	N/A	49	>700 mAh g^{-1} (100 cycles, 0.1 C)	[112a]
	Polysulfide-rich electrolyte passivated Li foil	$\approx 20 \mu\text{m}$	2 mg cm^{-2}	50	>700 mAh g^{-1} (100 cycles, 0.2 C)	[113]
	LaNO_3 electrolyte additive supported Li foil	24 μm	0.9 mg cm^{-2}	49	553 mAh g^{-1} (100 cycles, 0.2 C)	[17]
	Implantable solid electrolyte interphase supported Li metal	13.6 nm	1.1 mg cm^{-2}	63 (composites)	677 mAh g^{-1} (600 cycles, 1 C)	[112c]

artificial coating and interlayer materials, which are produced via physical or chemical treatments prior to battery assembly; and ii) in situ formed coating materials, which are formed during electrochemical processes. Detailed coating information and cell performance are summarized in Table 3.

4.1. Preformed Artificial Coating and Interlayer Materials for Li Protection

Research regarding lithium protection for Li–S batteries can be traced back to nearly 20 years ago. Pioneering work in this area aimed to use chemical approaches to passivate the surface of lithium. In 2003, Park and co-workers reported the use of a polymer coating on lithium for use in Li–S batteries.^[109] The polymer coating was formed via UV curing after dipping the lithium metal in a monomer solution of ethylene glycol dimethacrylate. The author demonstrated that the Li–S batteries using the protected Li anodes had a stable cycle life with a discharge capacity of 270 mAh g^{-1} . With the prosperity of Li–S batteries, lithium protection is considered to be a crucial aspect toward the practical application, and thereby novel coating materials have emerged for lithium protection.^[110] Wu and co-workers reported the use of a highly ionically conductive Li_3N thin-film coating on lithium anodes in Li–S batteries,^[107] prepared via a reaction between N_2 gas flowing over lithium metal. As shown in Figure 9a, the author claimed that the Li_3N coating layer protects the lithium foil from the side reactions between electrolyte and polysulfides, which improves the cycling stability of Li–S batteries. Gao and co-workers reported porous Al_2O_3 coatings on lithium anodes synthesized via a slurry paste method.^[111] With the coated lithium foil as an anode, side reactions from soluble polysulfides are suppressed with little deposition of insulating sulfides during cycling, ensuring improved

electrochemical activity and cycling stability of the lithium anode. Unfortunately, it is difficult to control the thickness and uniformity of coating layers precisely on Li metal using the aforementioned approaches, resulting in micrometer-scale coating thicknesses of the developed coatings. Additionally, the interaction between the coating layer and lithium metal is weak via a physical approach, which may impact the ionic conductivity of the Li anode. As previously mentioned, ALD and MLD techniques enable precise control of the thickness of coating layers at an atomic or molecular level, which can easily maintain the high ionic conductivity of the Li anode. Rubloff and co-workers first employed ALD Al_2O_3 as a coating for lithium anodes, as shown in Figure 9b.^[16] The authors determined that a 14 nm ultrathin ALD Al_2O_3 layer protects the lithium metal from side reactions with the dissolved polysulfides and electrolyte solvents. Compared with bare Li metal, the ALD Al_2O_3 -coated Li metal maintained the metal brightness after long time exposing in air and electrolyte, confirming the strong protection by the ALD thin film. The Li–S batteries demonstrate improved performance using ALD Al_2O_3 -coated Li anodes compared with the batteries using bare Li metal. It should be highlighted that the ALD technique can be applied not only to lithium metal, but also to other metal-based anodes as a protection layer, such as Na, Mg, and Al. The development of highly conductive freestanding interlayer structures is an attractive strategy for the protection of sulfur cathodes, and this method can also be applied to the protection of Li metal anodes. Sun and co-workers recently proposed a novel and universal approach to achieve long-lasting and dendrite-free Li metal anodes by introducing commercial carbon paper as an interlayer, as shown in Figure 9c.^[108] The developed Li anode with carbon paper interlayer in carbonate-based electrolytes in Li–S batteries has demonstrated excellent performance with improved Li-ion transportation, providing new avenues for the realization of next-generation high energy density Li metal batteries.

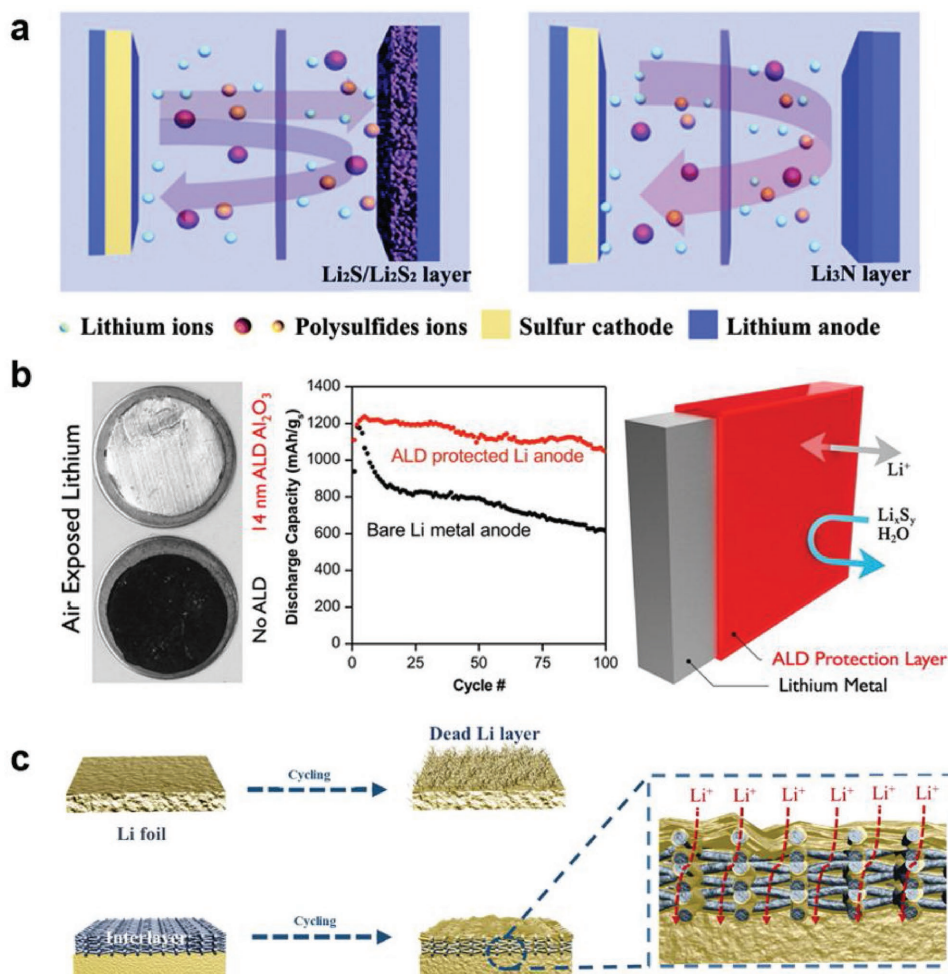


Figure 9. Artificial coating and interlayer materials for lithium anode in Li-S batteries: a) Li_3N coating. Reproduced with permission.^[107] Copyright 2014, Royal Society of Chemistry. b) ALD Al_2O_3 coating. Reproduced with permission.^[16] Copyright 2015, American Chemical Society. c) Freestanding carbon interlayer on lithium anodes. Reproduced with permission.^[108] Copyright 2018, Elsevier.

4.2. In Situ Formed Coating for Li Protection

In contrast to the preformed coating materials, in situ synthesis of coating materials is always accompanied by electrochemical reactions within the battery, and thus electrolyte optimization is the key for the development and tuning of film properties.^[17,112] The introduced electrolyte additives mainly have three functions: 1) reacting with decomposed electrolytes to form a smooth and stable interlayer; 2) trapping polysulfides to avoid the corrosion of lithium metal; and 3) preventing the growth of lithium dendrites. LiNO_3 is the most employed additive used in the ether-based electrolytes of Li-S batteries. It has been found that the surface of the lithium anode can be passivated by introducing LiNO_3 , preventing direct contact between the anode and dissolved polysulfides. In addition to LiNO_3 , other metal nitrides are also adopted as additives in ether-based electrolytes. As shown in **Figure 10a**, Gao and co-workers reported LaNO_3 as an additive in Li-S electrolytes which formed a $\text{La}_2\text{S}_3/\text{Li}_2\text{S}_2/\text{Li}_2\text{S}/\text{Li}_x\text{SO}_y$ interlayer as a protection layer for Li metal anodes.^[17] The author claimed that the La^{3+} cations are stable due to the large ionic radius, and are not strong enough to

catalyze the ring-opening polymerization of ether-based solvents due to the small ratio between ionic charge and ionic radius ($e^- \text{Å}^{-1}$) for La^{3+} cations as compared with other divalent and multivalent cations. Amine and co-workers^[112a] and Zu and Manthiram^[113] also reported different additives in electrolytes to form new interlayers for lithium metal protection in Li-S batteries.

In addition to employing electrolyte additives to form an SEI thin film, Zhang and co-workers developed an implantable SEI coating on a Li metallic anode via an electroplating strategy, as shown in **Figure 10b**.^[112c] The implantable SEI is formed by precycling Li metal in a lithium bis(trifluoromethylsulfonyl)imide (LiTFSI)- LiNO_3 - Li_2S_5 electrolyte. The SEI-modified Li anode demonstrates excellent performance in both ether- and carbonate-based electrolyte systems. Li-S pouch cells with the implantable SEI exhibit an improved discharge capacity from 156 to 917 mAh g^{-1} and enhanced Coulombic efficiency from 12% to 85% at 0.1 C. Compared to preformed artificial coating materials, in situ synthesis of coating materials is more simple and facile. However, the underlying mechanisms of the formation and reactions of in situ coatings are complicated and require further in-depth understanding.

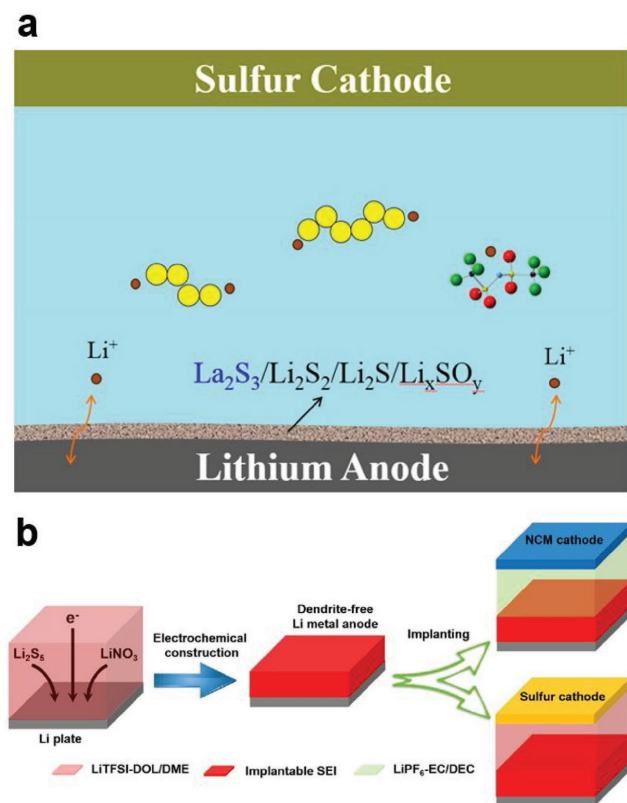


Figure 10. In situ formed coating for lithium anode in Li–S batteries: a) LaNO_3 electrolyte additive. Reproduced with permission.^[17] Copyright 2016, American Chemical Society. b) Implantable SEI layer for lithium anodes. Reproduced with permission.^[112c] Copyright 2017, Elsevier.

As a brief summary, the designed interface between the lithium anode and electrolyte aims to have high ionic conductivity for Li-ion transportation as well as high stability to prevent side reactions. Many preformed artificial coating materials, including carbon-based coatings and ALD metal-oxide coatings, have been developed to protect lithium anodes in Li–S batteries. For in situ coating materials, electrolyte additives are popular strategies to trigger the in situ coating formation toward the safe use of lithium metal in Li–S batteries. The development of a safe lithium anode is crucial to the development of high-energy Li–S batteries. However, the reported literature on the interface design of lithium anodes is still in its infancy, and many detailed studies and novel advanced designs will be required in the future.

5. Summary and Perspective

The development of Li–S batteries is an important direction on the road to high-energy storage devices. In this review, we summarize the design of interfaces and development of coatings and interlayers for Li–S batteries in the following:

1. *Development of Coating/Interlayer Materials:* Various coating materials and interlayer materials have been developed to overcome the challenges faced by sulfur cathodes. The

electronic and ionic conductivities, uniformity, controllable thickness, and other surface properties of these coating materials have been investigated in many reported references. The functions of these coating materials mainly focus on the localization of polysulfides, the improvement of whole electrode conductivity, and the accommodation of volume expansions. Most developed sulfur cathodes with coating materials have demonstrated to suppress the shuttle effect with reduced polysulfide dissolution, resulting in the improved cycling stability of Li–S batteries. On the other hand, there are still many unrevealed underlying mechanisms of coating materials. Carbon materials are the most prevailing coating materials. However, what kind of carbon materials is in favor as coating for sulfur cathodes is still inconclusive. For instance, there are mainly two viewpoints of the developed coating/interlayers towards polysulfides shuttle effect. One is the coating materials should be able to chemically or physically adsorb polysulfides. These materials either have very high surface area with porous structure to maintain the polysulfides and/or have surface electropositive properties to bond polysulfides. The adsorbed polysulfides in coating/interlayer matrix can be further utilized in the electrochemical reaction. Another viewpoint, conversely, is to build an electronegative surface to repel the polysulfides and force the polysulfides stay at cathode part. Until now, the above two mechanisms have not been determined which is more effective to solve the polysulfide shuttle issues. Furthermore, for adsorption/bonding effect between coating/interlayers and polysulfides, most of papers only give evidence on the bonding formation or the suppression of polysulfides dissolution with physical or electrochemical characterizations. However, the adsorption ability of various coating materials, such as hydrophobic/hydrophilic effect, crystalline/amorphous structure of metal oxides, thickness, and surface area of coating layer, is very rare to be determined, which needs more detailed and in-depth studies with advanced characterizations.

2. *Coating and Interlayer Structure Design:* As summarized in the context, the coating and interlayer structure can be mainly divided into two types: i) coating on individual composites and ii) thin-film coating (or freestanding interlayer inserting) on the whole electrodes. The two strategies have their own advantages and specificity. Coating materials on individual composites mostly have very delicate nanostructure with controllable morphology, such as yolk–shell structure. The mechanism of these coating materials is generally to confine the sulfur-active materials in the individual composites. Many advanced physical characterizations, such as TEM, synchrotron-based X-ray studies, NMR, UV, are used to demonstrate their structure, coating effect, and performances. However, synthesis of these coating materials is mostly in lab-scale and needs further development to confirm the future large-scale production potential. On the contrary, thin-film coating and freestanding interlayer for the whole electrodes are considered as very promising strategies for industry application due to their facile synthesis and easy scale-up process. Compared with the coating on individual composites, coating strategies on the whole electrodes are mostly in macroscopic scale and the coating/interlayer is in some extent considered as buffer layers to re-distribute the dissolved sulfur-active materials into

the coating matrix. Actually, due to the macroscopic structure, the characterization of these coating materials in the whole sulfur electrode is a challenge. More advanced characterizations, such as in situ X-ray tomography and X-ray imaging to investigate the adsorption process and distribution of polysulfides into the coating/interlayers can be further carried out and give more in-depth insights in the future.

3. *Li Anode Protection:* With the deeper understanding of Li–S batteries, an increasing number of researchers have moved toward the protection of lithium anodes. Especially coupling with high loading sulfur cathodes and operating at high rate, the utilization and protection of lithium metal are crucial to achieve high-energy and safe Li–S batteries. Many novel interface designs and elaborate coating materials have been reported in the metal protection and demonstrated excellent performance in the Li/Li stripping plating cell. However, very few protected Li anodes have been employed in Li–S batteries or other real Li-based batteries. Furthermore, compared with the interface studies of sulfur cathodes, the development of coating materials or interlayers on lithium anodes is still inadequate. Many underlying mechanisms of the Li anode in Li–S batteries and other energy storage systems are still unrevealed, which need advanced characterization techniques, such as in operando studies, to be fully explored in the future.
4. *ALD and MLD Thin-Film Coating:* ALD and MLD thin-film techniques received increasing attention within the fields of Li–S and Li-ion battery research. The novel structure, precise controllable thickness, and facile operation process of ALD/MLD are very promising for the development of advanced coating materials to address the needs of high-energy Li–S batteries. Furthermore, the ALD/MLD machines are easy to combine with glove box and other machines, which widen the application of these thin-film deposition techniques. As summarized from literature, ALD and MLD coating materials have been applied to sulfur cathodes, separators, and Li anodes in Li–S batteries. Especially for lithium protection, ALD and MLD thin-film techniques will certainly play a very large role in Li–S batteries in the near future. Furthermore, the development of roll-to-roll ALD machines and the investigation of ALD/MLD precursors will promote the practical application and reduce the high cost of ALD and MLD technique for batteries in future.
5. *Challenges of Coating Materials toward High-Energy Li–S Batteries:* High-energy Li–S batteries have been received extensive attention. To achieve the high energy density of over 300 Wh kg^{−1}, a single Li–S battery at least should have a high loading and high capacity sulfur cathode (>2 mg cm^{−2} sulfur), low electrolyte/sulfur ratio (<3:1), and a safe and stable Li anode. For the developed coating materials of sulfur-based nanocomposites, actually not many papers mentioned the performance of high loading sulfur cathodes in liquid based Li–S batteries. However, the delicate interphase design of these coated sulfur-based nanomaterials may play an important role for safe and high-energy all-solid-state Li–S batteries in the future to smooth the high interface resistances and improve the reaction kinetics of the solid-phase transformation. On the other hand, the reported literature with the coating/interlayer materials on the electrodes and

on separators has developed many high-loading sulfur cathodes with excellent performances. These reported papers mostly demonstrated stable and excellent electrochemical performance with very high sulfur loading, indicating the promising application in practical. However, there are still many issues to be addressed. First, the capacity calculation in reported literature is mostly based on sulfur active materials without the coating or interlayers in the batteries. These materials for sure will increase the inactive weight ratio of the whole battery. Even though the lightweight carbon-based interlayers will only occupy a very small ratio in the whole battery mass, electrolyte adsorption by these carbon materials will also increase and thereby the total energy densities of batteries are reduced. Therefore, the balance between the introduced carbon-based coating/interlayer materials and the total energy density of batteries will be an important direction in the development of high-energy Li–S batteries.

The development of Li–S batteries has spanned over a number of decades. Addressing the challenges at the interfaces is crucial for meeting the needs of high-energy Li–S batteries. This review summarized various coatings and interlayer materials developed at interfaces of Li–S batteries. These developed nanostructures and materials are very promising strategies to overcome such challenges and the investigation of interface modification with advanced characterization techniques provide an in-depth understanding on the design of high-energy Li–S batteries. These novel interface designs are not only limited to Li–S batteries but can also be applied to many other energy storage systems as well to further develop the field of clean energy storage.

Acknowledgements

This research was supported by Natural Sciences and Engineering Research Council of Canada (NSERC), Canada Research Chair Program (CRC), Canada Foundation for Innovation (CFI), Ontario Research Fund, and the University of Western Ontario. Thanks Alicia Koo for comments and editing. The authors declare no competing financial interests.

Conflict of Interest

The authors declare no conflict of interest.

Keywords

coating materials, interfaces, interlayer materials, lithium–sulfur batteries

Received: February 20, 2018

Revised: April 9, 2018

Published online:

-
- [1] a) P. G. Bruce, S. A. Freunberger, L. J. Hardwick, J. M. Tarascon, *Nat. Mater.* **2012**, *11*, 19; b) S. Evers, L. F. Nazar, *Acc. Chem. Res.* **2013**, *46*, 1135; c) M. K. Song, E. J. Cairns, Y. Zhang, *Nanoscale* **2013**, *5*, 2186.

- [2] a) Y. X. Yin, S. Xin, Y. G. Guo, L. J. Wan, *Angew. Chem.* **2013**, *52*, 13186; b) X.-P. Gao, H.-X. Yang, *Energy Environ. Sci.* **2010**, *3*, 174; c) N. Mahmood, Y. Hou, *Adv. Sci.* **2014**, *1*, 1400012.
- [3] a) J. Wang, Y. Li, X. Sun, *Nano Energy* **2013**, *2*, 443; b) D. Bresser, S. Passerini, B. Scrosati, *Chem. Commun.* **2013**, *49*, 10545; c) S. Wu, R. Ge, M. Lu, R. Xu, Z. Zhang, *Nano Energy* **2015**, *15*, 379.
- [4] a) Z. Li, Y. Huang, L. Yuan, Z. Hao, Y. Huang, *Carbon* **2015**, *92*, 41; b) M. A. Pope, I. A. Aksay, *Adv. Energy Mater.* **2015**, *5*, 1500124; c) J. Fang, F. Qin, J. Li, K. Zhang, W. Liu, M. Wang, F. Yu, L. Zhang, *J. Power Sources* **2015**, *297*, 265.
- [5] R. Cao, W. Xu, D. Lv, J. Xiao, J.-G. Zhang, *Adv. Energy Mater.* **2015**, *5*, 1402273.
- [6] L. Chen, L. L. Shaw, *J. Power Sources* **2014**, *267*, 770.
- [7] Z. Lin, C. Liang, *J. Mater. Chem. A* **2015**, *3*, 936.
- [8] a) J. Lim, J. Pyun, K. Char, *Angew. Chem.* **2015**, *54*, 3249; b) A. Manthiram, Y. Fu, S. H. Chung, C. Zu, Y. S. Su, *Chem. Rev.* **2014**, *114*, 11751.
- [9] a) M. Liu, F. Ye, W. Li, H. Li, Y. Zhang, *Nano Res.* **2016**, *9*, 94; b) Q. Pang, X. Liang, C. Y. Kwok, L. F. Nazar, *J. Electrochem. Soc.* **2015**, *162*, A2567; c) X. Fang, H. Peng, *Small* **2015**, *11*, 1488; d) S. S. Zhang, *Front. Energy Res.* **2013**, *1*, 10; e) J. Scheers, S. Fantini, P. Johansson, *J. Power Sources* **2014**, *255*, 204; f) R. Xu, J. Lu, K. Amine, *Adv. Energy Mater.* **2015**, *5*, 1500408; g) Z. Tu, P. Nath, Y. Lu, M. D. Tikekar, L. A. Archer, *Acc. Chem. Res.* **2015**, *48*, 2947.
- [10] X. Yao, N. Huang, F. Han, Q. Zhang, H. Wan, J. P. Muzerwa, C. Wang, X. Xu, *Adv. Energy Mater.* **2017**, *7*, 1602923.
- [11] J. Liang, Z.-H. Sun, F. Li, H.-M. Cheng, *Energy Storage Mater.* **2016**, *2*, 76.
- [12] Y. Yang, G. Yu, J. J. Cha, H. Wu, M. Vosgueritchian, Y. Yao, Z. Bao, Y. Cui, *ACS Nano* **2011**, *5*, 9187.
- [13] X. Li, A. Lushington, Q. Sun, W. Xiao, J. Liu, B. Wang, Y. Ye, K. Nie, Y. Hu, Q. Xiao, R. Li, J. Guo, T. K. Sham, X. Sun, *Nano Lett.* **2016**, *16*, 3545.
- [14] H. Yao, K. Yan, W. Li, G. Zheng, D. Kong, Z. W. Seh, V. K. Narasimhan, Z. Liang, Y. Cui, *Energy Environ. Sci.* **2014**, *7*, 3381.
- [15] Y. S. Su, A. Manthiram, *Nat. Commun.* **2012**, *3*, 1166.
- [16] A. C. Kozen, C. F. Lin, A. J. Pearce, M. A. Schroeder, X. Han, L. Hu, S. B. Lee, G. W. Rubloff, M. Noked, *ACS Nano* **2015**, *9*, 5884.
- [17] S. Liu, G. R. Li, X. P. Gao, *ACS Appl. Mater. Interfaces* **2016**, *8*, 7783.
- [18] a) R. Younesi, G. M. Veith, P. Johansson, K. Edström, T. Vegge, *Energy Environ. Sci.* **2015**, *8*, 1905; b) S. Zhang, K. Ueno, K. Dokko, M. Watanabe, *Adv. Energy Mater.* **2015**, *5*, 1500117.
- [19] a) G. He, S. Evers, X. Liang, M. Cuisinier, A. Garsuch, L. F. Nazar, *ACS Nano* **2013**, *7*, 10920; b) X. Ji, K. T. Lee, L. F. Nazar, *Nat. Mater.* **2009**, *8*, 500.
- [20] J. Liu, X. Sun, *Nanotechnology* **2015**, *26*, 024001.
- [21] a) X. Li, J. Liu, M. N. Banis, A. Lushington, R. Li, M. Cai, X. Sun, *Energy Environ. Sci.* **2014**, *7*, 768; b) J. B. Goodenough, Y. Kim, *J. Power Sources* **2011**, *196*, 6688; c) K. T. Lee, S. Jeong, J. Cho, *Acc. Chem. Res.* **2013**, *46*, 1161.
- [22] Y. Yang, G. Zheng, Y. Cui, *Chem. Soc. Rev.* **2013**, *42*, 3018.
- [23] a) Y.-J. Choi, Y.-D. Chung, C.-Y. Baek, K.-W. Kim, H.-J. Ahn, J.-H. Ahn, *J. Power Sources* **2008**, *184*, 548; b) N. Li, M. Zheng, H. Lu, Z. Hu, C. Shen, X. Chang, G. Ji, J. Cao, Y. Shi, *Chem. Commun.* **2012**, *48*, 4106; c) S. Lu, Y. Cheng, X. Wu, J. Liu, *Nano Lett.* **2013**, *13*, 2485; d) J. Rong, M. Ge, X. Fang, C. Zhou, *Nano Lett.* **2014**, *14*, 473.
- [24] F. Wu, J. Chen, R. Chen, S. Wu, L. Li, S. Chen, T. Zhao, *J. Phys. Chem. C* **2011**, *115*, 6057.
- [25] G.-C. Li, G.-R. Li, S.-H. Ye, X.-P. Gao, *Adv. Energy Mater.* **2012**, *2*, 1238.
- [26] H. Wang, Y. Yang, Y. Liang, J. T. Robinson, Y. Li, A. Jackson, Y. Cui, H. Dai, *Nano Lett.* **2011**, *11*, 2644.
- [27] S. Evers, L. F. Nazar, *Chem. Commun.* **2012**, *48*, 1233.
- [28] C. Nan, Z. Lin, H. Liao, M. K. Song, Y. Li, E. J. Cairns, *J. Am. Chem. Soc.* **2014**, *136*, 4659.
- [29] L. Suo, Y. Zhu, F. Han, T. Gao, C. Luo, X. Fan, Y.-S. Hu, C. Wang, *Nano Energy* **2015**, *13*, 467.
- [30] K. T. Lee, R. Black, T. Yim, X. Ji, L. F. Nazar, *Adv. Energy Mater.* **2012**, *2*, 1490.
- [31] X. Wang, G. Li, J. Li, Y. Zhang, A. Wook, A. Yu, Z. Chen, *Energy Environ. Sci.* **2016**, *9*, 2533.
- [32] Z. Wei Seh, W. Li, J. J. Cha, G. Zheng, Y. Yang, M. T. McDowell, P. C. Hsu, Y. Cui, *Nat. Commun.* **2013**, *4*, 1331.
- [33] W. Li, G. Zheng, Y. Yang, Z. W. Seh, N. Liu, Y. Cui, *Proc. Natl. Acad. Sci. USA* **2013**, *110*, 7148.
- [34] a) X. Li, X. Li, M. N. Banis, B. Wang, A. Lushington, X. Cui, R. Li, T.-K. Sham, X. Sun, *J. Mater. Chem. A* **2014**, *2*, 12866; b) B. Zhang, X. Qin, G. R. Li, X. P. Gao, *Energy Environ. Sci.* **2010**, *3*, 1531; c) K. Xi, S. Cao, X. Peng, C. Ducati, R. V. Kumar, A. K. Cheetham, *Chem. Commun.* **2013**, *49*, 2192.
- [35] a) Y. Shi, L. Peng, Y. Ding, Y. Zhao, G. Yu, *Chem. Soc. Rev.* **2015**, *44*, 6684; b) S. Dutta, A. Bhaumik, K. C. W. Wu, *Energy Environ. Sci.* **2014**, *7*, 3574.
- [36] a) K. R. Phillips, G. T. England, S. Sunny, E. Shirman, T. Shirman, N. Vogel, J. Aizenberg, *Chem. Soc. Rev.* **2016**, *45*, 281; b) G. Zhou, F. Li, H.-M. Cheng, *Energy Environ. Sci.* **2014**, *7*, 1307.
- [37] W. Li, Q. Zhang, G. Zheng, Z. W. Seh, H. Yao, Y. Cui, *Nano Lett.* **2013**, *13*, 5534.
- [38] a) L. Wang, Z. Dong, D. Wang, F. Zhang, J. Jin, *Nano Lett.* **2013**, *13*, 6244; b) L. Wang, X. He, J. Li, J. Gao, J. Guo, C. Jiang, C. Wan, *J. Mater. Chem.* **2012**, *22*, 22077; c) Y. Fu, A. Manthiram, *Chem. Mater.* **2012**, *24*, 3081; d) M. J. Lacey, F. Jeschull, K. Edstrom, D. Brandell, *Chem. Commun.* **2013**, *49*, 8531.
- [39] a) F. Wu, J. Chen, L. Li, T. Zhao, R. Chen, *J. Phys. Chem. C* **2011**, *115*, 24411; b) M. Kazazi, M. R. Vaezi, A. Kazemzadeh, *Ionics* **2013**, *20*, 635; c) J. Wang, L. Lu, D. Shi, R. Tandiono, Z. Wang, K. Konstantinov, H. Liu, *ChemPlusChem* **2013**, *78*, 318; d) X. Li, M. Rao, D. Chen, H. Lin, Y. Liu, Y. Liao, L. Xing, W. Li, *Electrochim. Acta* **2015**, *166*, 93.
- [40] J.-Q. Huang, Q. Zhang, S.-M. Zhang, X.-F. Liu, W. Zhu, W.-Z. Qian, F. Wei, *Carbon* **2013**, *58*, 99.
- [41] a) D. Higgins, P. Zamani, A. Yu, Z. Chen, *Energy Environ. Sci.* **2016**, *9*, 357; b) S. Xin, Y. G. Guo, L. J. Wan, *Acc. Chem. Res.* **2012**, *45*, 1759; c) Y. Zhao, X. Li, B. Yan, D. Xiong, D. Li, S. Lawes, X. Sun, *Adv. Energy Mater.* **2016**, *6*, 1502175.
- [42] a) V. Georgakilas, J. N. Tiwari, K. C. Kemp, J. A. Perman, A. B. Bourlinos, K. S. Kim, R. Zboril, *Chem. Rev.* **2016**, *116*, 5464; b) N. Karousis, I. Suarez-Martinez, C. P. Ewels, N. Tagmatarchis, *Chem. Rev.* **2016**, *116*, 4850.
- [43] Y. Hwa, J. Zhao, E. J. Cairns, *Nano Lett.* **2015**, *15*, 3479.
- [44] a) T. Yang, X. Wang, D. Wang, S. Li, D. Xie, X. Zhang, X. Xia, J. Tu, *J. Mater. Chem. A* **2016**, *4*, 16653; b) F. Wu, J. T. Lee, E. Zhao, B. Zhang, G. Yushin, *ACS Nano* **2016**, *10*, 1333; c) C. Chen, D. Li, L. Gao, P. P. R. M. L. Harks, R.-A. Eichel, P. H. L. Notten, *J. Mater. Chem. A* **2017**, *5*, 1428.
- [45] W. Zhou, X. Xiao, M. Cai, L. Yang, *Nano Lett.* **2014**, *14*, 5250.
- [46] Z. Xiao, Z. Yang, L. Wang, H. Nie, M. Zhong, Q. Lai, X. Xu, L. Zhang, S. Huang, *Adv. Mater.* **2015**, *27*, 2891.
- [47] W. Liu, J. Jiang, K. R. Yang, Y. Mi, P. Kumaravadivel, Y. Zhong, Q. Fan, Z. Weng, Z. Wu, J. J. Cha, H. Zhou, V. S. Batista, G. W. Brudvig, H. Wang, *Proc. Natl. Acad. Sci. USA* **2017**, *114*, 3578.
- [48] S. Niu, W. Lv, G. Zhou, H. Shi, X. Qin, C. Zheng, T. Zhou, C. Luo, Y. Deng, B. Li, F. Kang, Q.-H. Yang, *Nano Energy* **2016**, *30*, 138.

- [49] a) W. Sun, X. Ou, X. Yue, Y. Yang, Z. Wang, D. Rooney, K. Sun, *Electrochim. Acta* **2016**, *207*, 198; b) L. Wang, Z. Yang, H. Nie, C. Gu, W. Hua, X. Xu, X. a. Chen, Y. Chen, S. Huang, *J. Mater. Chem. A* **2016**, *4*, 15343.
- [50] X. Meng, X. Q. Yang, X. Sun, *Adv. Mater.* **2012**, *24*, 3589.
- [51] H. Kim, J. T. Lee, D.-C. Lee, A. Magasinski, W.-i. Cho, G. Yushin, *Adv. Energy Mater.* **2013**, *3*, 1308.
- [52] a) A. A. Dameron, D. Seghete, B. B. Burton, S. D. Davidson, A. S. Cavanagh, J. A. Bertrand, S. M. George, *Chem. Mater.* **2008**, *20*, 3315; b) S. M. George, *Chem. Rev.* **2010**, *110*, 111; c) C. N. McMahon, L. Alemany, R. L. Callender, S. G. Bott, A. R. Barron, *Chem. Mater.* **1999**, *11*, 3181.
- [53] a) H. Im, N. J. Wittenberg, N. C. Lindquist, S. H. Oh, *J. Mater. Res.* **2012**, *27*, 663; b) J. Liu, X. Meng, Y. Hu, D. Geng, M. N. Banis, M. Cai, R. Li, X. Sun, *Carbon* **2013**, *52*, 74; c) R. L. Puurunen, *J. Appl. Phys.* **2005**, *97*, 121301.
- [54] a) D. Wang, J. Yang, J. Liu, X. Li, R. Li, M. Cai, T.-K. Sham, X. Sun, *J. Mater. Chem. A* **2014**, *2*, 2306; b) J. Liu, M. N. Banis, Q. Sun, A. Lushington, R. Li, T. K. Sham, X. Sun, *Adv. Mater.* **2014**, *26*, 6472; c) X. Li, X. Meng, J. Liu, D. Geng, Y. Zhang, M. N. Banis, Y. Li, J. Yang, R. Li, X. Sun, M. Cai, M. W. Verbrugge, *Adv. Funct. Mater.* **2012**, *22*, 1647; d) A. Lushington, J. Liu, Y. Tang, R. Li, X. Sun, *J. Vac. Sci. Technol., A* **2014**, *32*, 01A124.
- [55] S. M. George, B. Yoon, A. A. Dameron, *Acc. Chem. Res.* **2009**, *42*, 498.
- [56] a) X. Li, J. Liu, B. Wang, M. N. Banis, B. Xiao, R. Li, T.-K. Sham, X. Sun, *RSC Adv.* **2014**, *4*, 27126; b) M. Yu, W. Yuan, C. Li, J.-D. Hong, G. Shi, *J. Mater. Chem. A* **2014**, *2*, 7360.
- [57] X. Li, A. Lushington, J. Liu, R. Li, X. Sun, *Chem. Commun.* **2014**, *50*, 9757.
- [58] B. Yoon, D. Seghete, A. S. Cavanagh, S. M. George, *Chem. Mater.* **2009**, *21*, 5365.
- [59] a) D. M. Piper, J. J. Travis, M. Young, S. B. Son, S. C. Kim, K. H. Oh, S. M. George, C. Ban, S. H. Lee, *Adv. Mater.* **2014**, *26*, 1596; b) H. Kim, J. T. Lee, G. Yushin, *J. Power Sources* **2013**, *226*, 256.
- [60] a) B. Scrosati, J. Hassoun, Y.-K. Sun, *Energy Environ. Sci.* **2011**, *4*, 3287; b) L. Lu, X. Han, J. Li, J. Hua, M. Ouyang, *J. Power Sources* **2013**, *226*, 272.
- [61] C. Li, S. Dong, D. Guo, Z. Zhang, M. Wang, L. Yin, *Electrochim. Acta* **2017**, *251*, 43.
- [62] Y. Deng, H. Xu, Z. Bai, B. Huang, J. Su, G. Chen, *J. Power Sources* **2015**, *300*, 386.
- [63] J. Wang, J. Chen, K. Konstantinov, L. Zhao, S. H. Ng, G. X. Wang, Z. P. Guo, H. K. Liu, *Electrochim. Acta* **2006**, *51*, 4634.
- [64] Y. Fu, A. Manthiram, *J. Phys. Chem. C* **2012**, *116*, 8910.
- [65] G. Ma, Z. Wen, J. Jin, Y. Lu, K. Rui, X. Wu, M. Wu, J. Zhang, *J. Power Sources* **2014**, *254*, 353.
- [66] K. Park, J. H. Cho, J.-H. Jang, B.-C. Yu, A. T. De La Hoz, K. M. Miller, C. J. Ellison, J. B. Goodenough, *Energy Environ. Sci.* **2015**, *8*, 2389.
- [67] Y. Cao, X. Li, I. A. Aksay, J. Lemmon, Z. Nie, Z. Yang, J. Liu, *Phys. Chem. Chem. Phys.* **2011**, *13*, 7660.
- [68] D.-h. Wang, D. Xie, X.-h. Xia, X.-q. Zhang, W.-j. Tang, Y. Zhong, J.-b. Wu, X.-l. Wang, J.-p. Tu, *J. Mater. Chem. A* **2017**, *5*, 19358.
- [69] H. Wang, S. Li, D. Li, Z. Chen, H. K. Liu, Z. Guo, *Energy* **2014**, *75*, 597.
- [70] a) S.-H. Chung, A. Manthiram, *Adv. Funct. Mater.* **2014**, *24*, 5299; b) H. Wei, J. Ma, B. Li, Y. Zuo, D. Xia, *ACS Appl. Mater. Interfaces* **2014**, *6*, 20276; c) H. Wang, W. Zhang, H. Liu, Z. Guo, *Angew. Chem.* **2016**, *55*, 3992.
- [71] G. Zhou, S. Pei, L. Li, D. W. Wang, S. Wang, K. Huang, L. C. Yin, F. Li, H. M. Cheng, *Adv. Mater.* **2014**, *26*, 625.
- [72] Z. Du, C. Guo, L. Wang, A. Hu, S. Jin, T. Zhang, H. Jin, Z. Qi, S. Xin, X. Kong, Y. G. Guo, H. Ji, L. J. Wan, *ACS Appl. Mater. Interfaces* **2017**, *9*, 43696.
- [73] W. Li, J. Hicks-Garner, J. Wang, J. Liu, A. F. Gross, E. Sherman, J. Graetz, J. J. Vajo, P. Liu, *Chem. Mater.* **2014**, *26*, 3403.
- [74] R. Song, R. Fang, L. Wen, Y. Shi, S. Wang, F. Li, *J. Power Sources* **2016**, *301*, 179.
- [75] M. S. Kim, L. Ma, S. Choudhury, L. A. Archer, *Adv. Mater. Interfaces* **2016**, *3*, 1600450.
- [76] S. H. Chung, A. Manthiram, *Adv. Mater.* **2014**, *26*, 7352.
- [77] G. Zhou, L. Li, D. W. Wang, X. Y. Shan, S. Pei, F. Li, H. M. Cheng, *Adv. Mater.* **2015**, *27*, 641.
- [78] a) S. H. Chung, A. Manthiram, *J. Phys. Chem. Lett.* **2014**, *5*, 1978; b) X. Cheng, W. Wang, A. Wang, K. Yuan, Z. Jin, Y. Yang, X. Zhao, *RSC Adv.* **2016**, *6*, 89972; c) B. Liu, X. Wu, S. Wang, Z. Tang, Q. Yang, G. H. Hu, C. Xiong, *Nanomaterials* **2017**, *7*, 196; d) H. Wu, Y. Huang, W. Zhang, X. Sun, Y. Yang, L. Wang, M. Zong, *J. Alloys Compd.* **2017**, *708*, 743; e) X. Sun, J. Wang, X. Li, W. Chen, *J. Nanopart. Res.* **2018**, *20*, 13.
- [79] S. H. Chung, P. Han, A. Manthiram, *ACS Appl. Mater. Interfaces* **2016**, *8*, 4709.
- [80] a) C.-H. Chang, S.-H. Chung, A. Manthiram, *J. Mater. Chem. A* **2015**, *3*, 18829; b) L. Luo, S.-H. Chung, A. Manthiram, *J. Mater. Chem. A* **2016**, *4*, 16805.
- [81] J. H. Kim, J. Seo, J. Choi, D. Shin, M. Carter, Y. Jeon, C. Wang, L. Hu, U. Paik, *ACS Appl. Mater. Interfaces* **2016**, *8*, 20092.
- [82] a) Q. Xu, G. C. Hu, H. L. Bi, H. F. Xiang, *Ionics* **2014**, *21*, 981; b) Y. Zhao, M. Liu, W. Lv, Y.-B. He, C. Wang, Q. Yun, B. Li, F. Kang, Q.-H. Yang, *Nano Energy* **2016**, *30*, 1; c) J. C. Bachman, S. Muy, A. Grimaud, H. H. Chang, N. Pour, S. F. Lux, O. Paschos, F. Maglia, S. Lupart, P. Lamp, L. Giordano, Y. Shao-Horn, *Chem. Rev.* **2016**, *116*, 140; d) G. Xu, Q.-b. Yan, S. Wang, A. Kushima, P. Bai, K. Liu, X. Zhang, Z. Tang, J. Li, *Chem. Sci.* **2017**, *8*, 6619.
- [83] M. S. Kim, L. Ma, S. Choudhury, S. S. Moganty, S. Wei, L. A. Archer, *J. Mater. Chem. A* **2016**, *4*, 14709.
- [84] Y. S. Su, A. Manthiram, *Chem. Commun.* **2012**, *48*, 8817.
- [85] S. H. Chung, A. Manthiram, *Chem. Commun.* **2014**, *50*, 4184.
- [86] X. Han, Y. Xu, X. Chen, Y.-C. Chen, N. Weadock, J. Wan, H. Zhu, Y. Liu, H. Li, G. Rubloff, C. Wang, L. Hu, *Nano Energy* **2013**, *2*, 1197.
- [87] a) R. Singhal, S.-H. Chung, A. Manthiram, V. Kalra, *J. Mater. Chem. A* **2015**, *3*, 4530; b) S. H. Chung, A. Manthiram, *Adv. Mater.* **2013**, *26*, 1360; c) S.-H. Chung, A. Manthiram, *Electrochim. Acta* **2013**, *107*, 569; d) Y. S. Su, Y. Fu, T. Cochell, A. Manthiram, *Nat. Commun.* **2013**, *4*, 2985; e) S.-H. Chung, A. Manthiram, *ChemSusChem* **2014**, *7*, 1655; f) G. Zhou, E. Paek, G. S. Hwang, A. Manthiram, *Nat. Commun.* **2015**, *6*, 7760.
- [88] a) Z. Ma, Z. Li, K. Hu, D. Liu, J. Huo, S. Wang, *J. Power Sources* **2016**, *325*, 71; b) G. Liang, J. Wu, X. Qin, M. Liu, Q. Li, Y. B. He, J. K. Kim, B. Li, F. Kang, *ACS Appl. Mater. Interfaces* **2016**, *8*, 23105.
- [89] X. Gu, C.-j. Tong, C. Lai, J. Qiu, X. Huang, W. Yang, B. Wen, L.-m. Liu, Y. Hou, S. Zhang, *J. Mater. Chem. A* **2015**, *3*, 16670.
- [90] C. Y. Fan, H. Y. Yuan, H. H. Li, H. F. Wang, W. L. Li, H. Z. Sun, X. L. Wu, J. P. Zhang, *ACS Appl. Mater. Interfaces* **2016**, *8*, 16108.
- [91] F. Wu, J. Qian, R. Chen, Y. Ye, Z. Sun, Y. Xing, L. Li, *J. Mater. Chem. A* **2016**, *4*, 17033.
- [92] T. Z. Zhuang, J. Q. Huang, H. J. Peng, L. Y. He, X. B. Cheng, C. M. Chen, Q. Zhang, *Small* **2016**, *12*, 381.
- [93] P.-Y. Zhai, H.-J. Peng, X.-B. Cheng, L. Zhu, J.-Q. Huang, W. Zhu, Q. Zhang, *Energy Storage Mater.* **2017**, *7*, 56.
- [94] R. Ponraj, A. G. Kannan, J. H. Ahn, J. H. Lee, J. Kang, B. Han, D. W. Kim, *ACS Appl. Mater. Interfaces* **2017**, *9*, 38445.
- [95] P. Zuo, J. Hua, M. He, H. Zhang, Z. Qian, Y. Ma, C. Du, X. Cheng, Y. Gao, G. Yin, *J. Mater. Chem. A* **2017**, *5*, 10936.

- [96] Q. Zeng, X. Leng, K.-H. Wu, I. R. Gentle, D.-W. Wang, *Carbon* **2015**, *93*, 611.
- [97] H. Deng, L. Yao, Q.-A. Huang, Q. Su, J. Zhang, G. Du, *Mater. Res. Bull.* **2016**, *84*, 218.
- [98] Q. Li, M. Liu, X. Qin, J. Wu, W. Han, G. Liang, D. Zhou, Y.-B. He, B. Li, F. Kang, *J. Mater. Chem. A* **2016**, *4*, 12973.
- [99] C.-H. Chang, S.-H. Chung, A. Manthiram, *Sustainable Energy Fuels* **2017**, *1*, 444.
- [100] D. K. Lee, C. W. Ahn, H.-J. Jeon, *J. Power Sources* **2017**, *360*, 559.
- [101] H. Li, L. Sun, Y. Zhang, T. Tan, G. Wang, Z. Bakenov, *J. Energy Chem.* **2017**, *26*, 1276.
- [102] K. Wu, Y. Hu, Z. Shen, R. Chen, X. He, Z. Cheng, P. Pan, *J. Mater. Chem. A* **2018**, *6*, 2693.
- [103] a) W. Xu, J. Wang, F. Ding, X. Chen, E. Nasybulin, Y. Zhang, J.-G. Zhang, *Energy Environ. Sci.* **2014**, *7*, 513; b) Z. Li, J. Huang, B. Yann Liaw, V. Metzler, J. Zhang, *J. Power Sources* **2014**, *254*, 168; c) X.-B. Cheng, J.-Q. Huang, Q. Zhang, *J. Electrochem. Soc.* **2017**, *165*, A6058.
- [104] a) C. Liang, M. Gao, H. Pan, Y. Liu, M. Yan, *J. Alloys Compd.* **2013**, *575*, 246; b) Y. Takeda, O. Yamamoto, N. Imanishi, *Electrochemistry* **2016**, *84*, 210.
- [105] a) L. Ji, M. Rao, H. Zheng, L. Zhang, Y. Li, W. Duan, J. Guo, E. J. Cairns, Y. Zhang, *J. Am. Chem. Soc.* **2011**, *133*, 18522; b) X. Gao, J. Li, D. Guan, C. Yuan, *ACS Appl. Mater. Interfaces* **2014**, *6*, 4154; c) R. Chen, T. Zhao, J. Lu, F. Wu, L. Li, J. Chen, G. Tan, Y. Ye, K. Amine, *Nano Lett.* **2013**, *13*, 4642.
- [106] D. Aurbach, E. Pollak, R. Elazari, G. Salitra, C. S. Kelley, J. Affinito, *J. Electrochem. Soc.* **2009**, *156*, A694.
- [107] G. Ma, Z. Wen, M. Wu, C. Shen, Q. Wang, J. Jin, X. Wu, *Chem. Commun.* **2014**, *50*, 14209.
- [108] Y. Zhao, Q. Sun, X. Li, C. Wang, Y. Sun, K. R. Adair, R. Li, X. Sun, *Nano Energy* **2018**, *43*, 368.
- [109] Y. M. Lee, N.-S. Choi, J. H. Park, J.-K. Park, *J. Power Sources* **2003**, *119–121*, 964.
- [110] a) S. j. Oh, W. y. Yoon, *Int. J. Precision Eng. Manuf.* **2014**, *15*, 1453; b) G. Ma, Z. Wen, Q. Wang, C. Shen, J. Jin, X. Wu, *J. Mater. Chem. A* **2014**, *2*, 19355.
- [111] H.-K. Jing, L.-L. Kong, S. Liu, G.-R. Li, X.-P. Gao, *J. Mater. Chem A* **2015**, *3*, 12213.
- [112] a) F. Wu, J. Qian, R. Chen, J. Lu, L. Li, H. Wu, J. Chen, T. Zhao, Y. Ye, K. Amine, *ACS Appl. Mater. Interfaces* **2014**, *6*, 15542; b) C. Zu, Y. Fu, A. Manthiram, *J. Mater. Chem. A* **2013**, *1*, 10362; c) X.-B. Cheng, C. Yan, X. Chen, C. Guan, J.-Q. Huang, H.-J. Peng, R. Zhang, S.-T. Yang, Q. Zhang, *Chem* **2017**, *2*, 258.
- [113] C. Zu, A. Manthiram, *J. Phys. Chem. Lett.* **2014**, *5*, 2522.